

# Enigmatic Red Beds Exposed at Point of Rocks, Cimarron National Grassland, Morton County, Kansas: Chronostratigraphic Constraints from Uranium-Lead Dating of Detrital Zircons

Jon J. Smith<sup>1</sup>, Brian F. Platt<sup>2</sup>, Greg A. Ludvigson<sup>1</sup>, Robert S. Sawin<sup>1</sup>,  
Craig P. Marshall<sup>3</sup>, and Alison Olcott-Marshall<sup>3</sup>

<sup>1</sup> *Kansas Geological Survey, 1930 Constant Avenue, Lawrence, Kansas 66047*

<sup>2</sup> *University of Mississippi, Department of Geology and Geological Engineering, 120A Carrier Hall,  
University, Mississippi, 38677*

<sup>3</sup> *The University of Kansas, Department of Geology, 1475 Jayhawk Blvd,  
Lawrence, Kansas 66045-7594*

## Abstract

Point of Rocks, a high-relief bluff overlooking the Cimarron River valley in Morton County, Kansas, is capped by distinct white beds of Neogene Ogallala Formation calcrete that overlie red beds of shale, siltstone, and sandstone. These unfossiliferous red beds are currently assigned to the Jurassic System; however, their age has long been debated due to a lack of marker beds, index fossils, and nearby correlative outcrops. As a result, geologists over the years have assigned the rocks to systems ranging from the Permian to the Cretaceous. In this study, four stratigraphic sections were measured in the red beds and three bulk samples were collected to determine the uranium-lead age distributions of detrital zircon (DZ) populations. Red-bed strata composed of fissile shale and sandstone are interpreted as alluvial overbank deposits, while dominantly trough cross-bedded and planar-laminated sandstones are interpreted as tidally influenced fluvial deposits. Detrital zircon age peaks can be grouped into at least seven subpopulations with a youngest single zircon age of  $263.8 \pm 12.1$  Ma, a more conservative age of  $293.0 \pm 6.95$  Ma based on the youngest grouping of three grain ages overlapping at  $2\sigma$ , and a complete absence of Mesozoic age zircons. In addition, copper oxides along partings and fractures suggest that the red beds once hosted copper sulfides, a common constituent of regional Permian-Triassic red beds. The DZ data—in conjunction with the identification of the Permian Day Creek Dolomite marker bed in logs of nearby drilling tests—strongly suggest that the enigmatic red beds cropping out at the base of Point of Rocks should be assigned to the Guadalupian Big Basin Formation, the uppermost Permian unit in Kansas.

## 1. Introduction

A prominent bluff in Morton County, Kansas, Point of Rocks was one of the best-known landmarks for 19<sup>th</sup>-century travelers on the Santa Fe Trail's Cimarron Cutoff, also called the Dry Route (fig. 1), because it signaled proximity to natural springs in a long stretch with few sources of water. Overlooking the Cimarron River valley, the south-facing bluff is capped by distinct white beds of Neogene Ogallala Formation calcrete. Older rocks underlying the Ogallala—red, tan, and gray beds of shale, siltstone, and sandstone—crop out for approximately 500 m along the base of the bluff (figs. 2 and 3). These red beds are currently assigned to the Jurassic System (Zeller, 1968)<sup>1</sup>. However, the rocks at this isolated exposure have always been problematic and, historically, have been classified as Triassic, Cretaceous, and Permian. Over the years, several geologists have examined the exposed red beds at the base of Point of

Rocks for fossils to help determine their age (Smith, 1940; Liggett and Zakrzewski, 1997; Liggett et al., 1998), but the rocks appear to be unfossiliferous. Speculation about their age has been based on correlation to lithologically similar rocks in Oklahoma, Colorado, and New Mexico, where the ages are known. This indirect approach has not provided a definitive solution. The purpose of this paper is to present the results of our study in which uranium-lead ages from detrital zircons were used to improve chronostratigraphic constraints on the deposition of red-bed strata at Point of Rocks.

Uranium-lead age distributions of populations of detrital zircons (DZ) within a sedimentary unit yield trends that represent the relative contributions of weathered igneous material from particular events or provinces (e.g., Dickinson and Gehrels, 2009, 2010; Dickinson et al., 2010). Comparisons of DZ age distributions between strata can reveal changes in source areas and drainage networks over

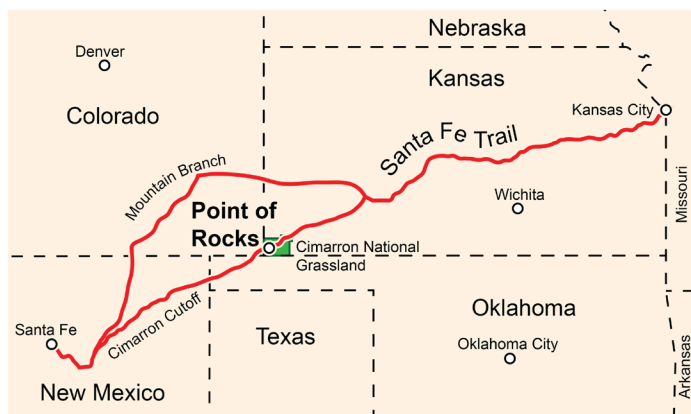


Figure 1. Map showing the historic Santa Fe Trail and the location of Point of Rocks in the Cimarron National Grassland, Morton County, southwestern Kansas.

time. The youngest uranium-lead ages of grains in DZ populations are commonly used to constrain maximum depositional ages (Dickinson and Gehrels, 2010). A growing database of DZ ages from various lithostratigraphic units offers opportunities to compare data from previously unknown samples when searching for similar provenance (Gehrels, 2012). After using this approach and examining previously overlooked subsurface data to constrain timing of deposition, we conclude that the enigmatic strata cropping out at the base of Point of Rocks are red beds of the Permian Big Basin Formation.

Results of this study solve a geological riddle that has existed since this exposure was first studied in the late 1800s and can be used to improve future geologic maps of the area, enhance regional stratigraphic correlations in the High Plains, and elucidate the duration of the pre-Ogallala unconformity in this area.

## 2. History of Stratigraphic Nomenclature

The depositional age of red beds at Point of Rocks has long been debated due to an absence of regional marker beds and index fossils. As a result, the rocks historically have been assigned to geological systems ranging from the Permian to the Cretaceous based on little more than lithologic similarities with distant potential correlatives (fig. 4). The first published mention of exposures at Point of Rocks was by Gould (1901) while describing isolated outcrops of the Dakota Group in the extreme southwestern corner of Kansas. He inferred a Triassic age for red beds in western Kansas based on similar strata in western Oklahoma containing invertebrate fossils, though such fossils were not reported from Kansas deposits. Moore and Landes (1937) in their *Geologic Map of Kansas* also showed Dakota Group and Triassic (?) red beds in the Point of Rocks area.

In a publication about the Permian red beds of Kansas, Norton (1939) suggested that “a small exposure in Morton County” (presumably referring to Point of Rocks) may be Big Basin Formation but offered no further evidence or explanation as to why he thought it might be Permian in age. Smith (1940) seemed to have deferred to Moore and Landes (1937) that the red beds are Triassic (?) but



Figure 2. Aerial photo showing the location of the red beds at the base of the bluff, the overlying Ogallala Formation, and the parking area (road loop) atop the Point of Rocks landmark (photo by William C. Johnson).

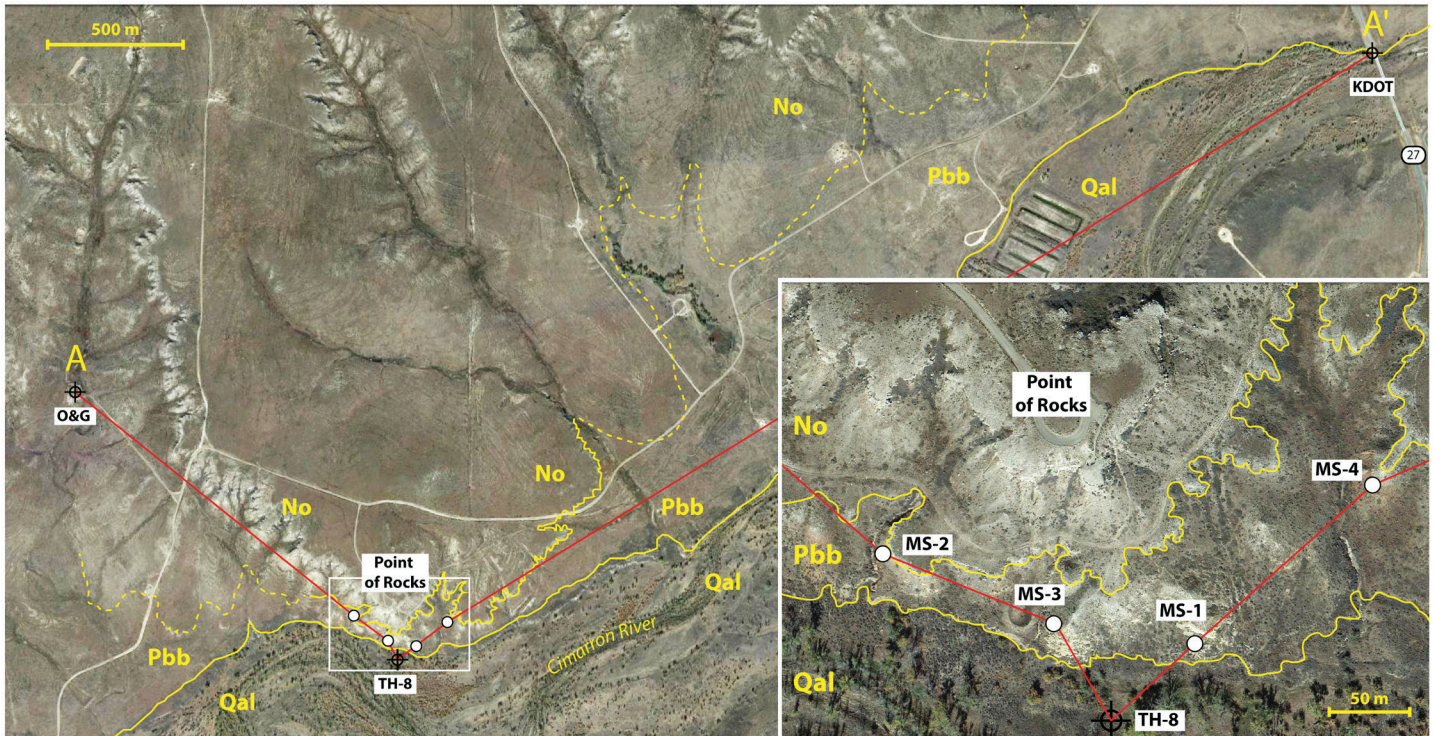


Figure 3. Aerial view of the study area (modified from Google Earth, accessed March 3, 2015) showing location of measured sections and drillers' logs used to construct cross section A–A' (fig. 13). Geologic contacts (yellow lines) between the Neogene Ogallala Formation (No), the Permian Big Basin Formation (Pbb), and Quaternary alluvium (Qal) are based on the results of this study and photo interpretation. Inset shows the locations of the measured sections (MS-1 to MS-4) and test hole 8 (McLaughlin, 1942; test hole 8, p. 108).

System	Series	Chronostratigraphic Interpretations						
		Gould (1901) Moore and Landes (1937)	Norton (1939)	Smith (1940)	McLaughlin (1942)	Moore et al. (1951, 1952)	Zeller (1968)	Proposed Chronostratigraphy (this study)
NEOGENE	Miocene	Ogallala Formation	Ogallala Formation	Ogallala Formation	Ogallala Formation	Ogallala Formation	Ogallala Formation	Ogallala Formation
CRETACEOUS	Upper	Dakota Formation						
	Lower			Cheyenne Sandstone				
JURASSIC	Upper						undifferentiated Jurassic rocks	
TRIASSIC	Upper	Triassic (?)		Triassic (?)	Dockum Group (?)	Dockum Group (?)		
PERMIAN	Guadalupian		Big Basin Formation					Big Basin Formation

Figure 4. Historical stratigraphic interpretations of strata in the Point of Rocks study area compared with the chronostratigraphy proposed in this study.

identified the overlying sandstone as the Lower Cretaceous Cheyenne Sandstone. McLaughlin (1942) classed the exposures at “Point Rock” (Point of Rocks) as Triassic (?), possibly Upper Triassic Dockum Group, and compared them lithologically to red beds exposed in the Red Point district in Texas County, Oklahoma. Moore et al. (1944) and Moore et al. (1951, 1952) classified the rocks as Triassic (?) Dockum group, an unnamed formation, and Triassic Dockum (?) Group, respectively, based on correlations with rocks of similar lithologies in Oklahoma, Texas, and New Mexico.

The most recently accepted stratigraphic guide and chart for Kansas by the KGS (Zeller, 1968) classified the exposure at Point of Rocks as Jurassic based on personal communications between the KGS’s Committee on Stratigraphic Nomenclature and E. D. Gutentag (USGS) in 1966 and 1967 (Sawin, 2015). Since Zeller was published in 1968, the age of the exposure has continued to be controversial, with various authors speculating about whether the rocks were Triassic (Kansas Geological Survey, 1991; McNinch, 1996; Liggett and Zakrzewski, 1997; Liggett et al., 1998; Croxton et al., 1998) or Jurassic (Kume and Spinazola, 1985; Johnson et al., 2009). None of these reports presented new evidence concerning the age of the exposed rocks and all were based on existing literature summarized herein.

### 3. Methods and Materials

Four stratigraphic sections were measured in the red beds at the base of Point of Rocks along the north wall of the Cimarron River valley (fig. 5). All units were measured with a Jacob staff and sighting level. Lithologic units were characterized in the field by color, grain size, composition, texture, and primary and secondary sedimentary structures. Color was described from fresh hand samples using Munsell color charts (Munsell Color, 2000).

Raman spectroscopy was used to determine the mineralogy of blue-tinted oxide coatings on red-bed shales near measured section MS-4. Standard point Raman spectra were collected from this rock sample with a Renishaw *inVia* Reflex Raman Microprobe using a Peltier cooled charge-coupled device camera (1024 x 256 pixels). The Raman light was dispersed by a diffraction grating with 2,400 mm/line and analyzed at room temperature. Sample excitation was achieved with an argon ion laser emitting at a wavelength of 514.5 nm. The laser power impinging on the samples was between 1 and 5 mW to minimize laser-induced heating of samples. Spectra were collected with a x20 (0.40 numerical aperture) objective lens for four accumulations of 20 s. Calibration of the Raman shift is achieved by recording the Raman spectrum of the silicon  $F_{1g}$  mode for one accumulation and 10 s. If necessary, an offset correction is performed to ensure that the position of the  $F_{1g}$  band is at  $520.50 \pm 0.10 \text{ cm}^{-1}$ .

Detrital zircons from three bulk sandstone samples (fig. 5; POR1-2, POR3-1, POR4-1) were analyzed using laser ablation–inductively coupled plasma–mass spectrometry (LA-ICP-MS) at the Arizona Laser-Chron Center using methods described by Gehrels et al. (2006, 2008). Reported ages are best age estimates, i.e., when the average of the  $^{238}\text{U}/^{206}\text{Pb}$  age and the  $^{207}\text{Pb}/^{206}\text{Pb}$  age is more than 1 Ga, the  $^{207}\text{Pb}/^{206}\text{Pb}$  age is reported. Ages less than 1 Ga are  $^{238}\text{U}/^{206}\text{Pb}$  ages. Analytical results are presented using features available in Ludwig (2012) and the NORMALIZED PROB PLOT, OVERLAP-SIMILARITY PROGRAM, and AGE PICK Excel macros listed in the Analysis Tools section of the Arizona Laser-Chron Center webpage ([www.laserchron.org](http://www.laserchron.org)). Maximum deposi-

tional ages are calculated using techniques outlined in Dickinson and Gehrels (2010) on the aggregated set of all detrital zircons sampled at Point of Rocks.

## 4.0 Results

### 4.1 Lithofacies

Five facies are recognized from the measured stratigraphic sections (fig. 5). The five facies are 1) fissile red beds, 2) structureless sandstone, 3) trough cross-bedded sandstone, 4) planar-laminated sandstone, and 5) mudstone clast conglomerate. We examined the outcrops for both body and trace fossils and, as with previous studies (Smith, 1940; Liggett and Zakrzewski, 1997; Liggett et al., 1998), none were found.

#### 4.1.1 Fissile red beds (figs. 6A–B; 7)

The fissile red beds facies is composed of thin beds of dark red (2.5YR 3/6) to reddish-brown (2.5YR 5/4), generally structureless, fissile siltstone interstratified with reddish-brown (2.5YR 5/4), very fine grained, feldspathic shale and sandstone (fig. 6A). This unit is laterally extensive and comprises the majority of strata in the study area, except in the area immediately below the Point of Rocks. Contacts with the overlying Ogallala are generally sharp, though in some areas horizontal and subvertical calcrete sheet cracks (2–20 cm thick) penetrate and accentuate bedding in the upper 2 m of the fissile red bed facies (fig. 6B). A thin blue varnish is present on many siltstone and shale partings in this facies (fig. 7). Raman spectra acquired in the mineral fingerprint region ( $100\text{--}1,800 \text{ cm}^{-1}$ ) from the blue-colored material in hand samples shows two broad bands between 500 and 650  $\text{cm}^{-1}$ . Based on the modes predicted by group theory analysis for copper-oxide cuprite ( $\text{Cu}_2\text{O}$ ; Williams and Porto, 1973), these two distinctive broad bands are assigned to copper oxide ( $\text{Cu}_2\text{O}$ ) at 580 and 630  $\text{cm}^{-1}$ .

#### 4.1.2 Structureless sandstone (figs. 6C–D)

The structureless sandstone facies is composed of thin to thick beds of tan (10YR 8/3; weathers reddish brown to yellow), very fine to fine-grained, well-cemented, predominantly subrounded quartz sandstone (fig. 6C). Sedimentary structures are absent or only weakly expressed. Dark red (2.5YR 3/6) mudstone clasts up to 10 cm in diameter occur in this facies but are rare (fig. 6D). Structureless sandstone beds are commonly interbedded with fissile siltstone. This facies ranges from 0.5 to 1.5 m thick, though actual bed thicknesses for this facies in particular are obscured by intervals of fine-grained talus derived most likely from weathered siltstones.

#### 4.1.3 Trough cross-bedded sandstone (figs. 8A–B)

Thick beds of trough cross-bedded sandstone are present in sections measured immediately underlying the Point of Rocks promontory (fig. 5; MS-1 and MS-3). This facies is composed of light gray (10YR 7/2) to tan (10YR 6/6), very fine to fine-grained, well-cemented, well-sorted quartz sandstone (fig. 8A). Cross-beds are approximately 1 cm thick and arranged in trough sets approximately 10 cm thick (fig. 8B). On weathered surfaces, calcareous cements may stand in positive relief as small knobby nodules or as thin (less than 1 cm) sheets along bedding planes and laminae. Trough axes are oriented in a roughly north-south direction with paleodrainage indicated toward the south.

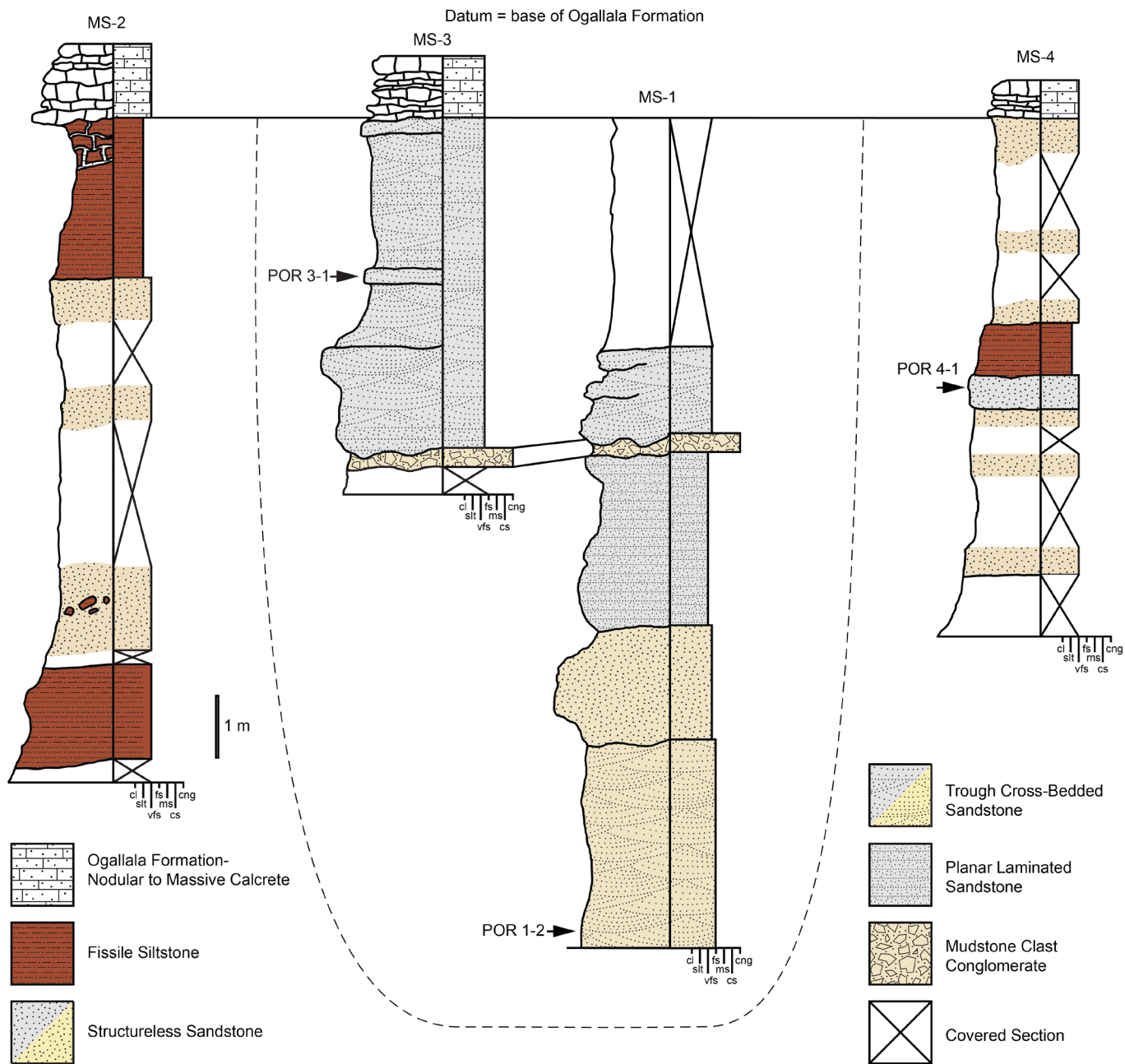


Figure 5. Measured sections at Point of Rocks showing the interpreted facies and stratigraphic positions of bulk samples collected for uranium-lead age dating of detrital zircons. Dashed line indicates our interpreted break in architectural elements separating the paleochannel deposits from the overbank sediments. Grain-size scale abbreviations: clay (cl), silt (slt), very fine sand (vfs), fine sand (fs), medium sand (ms), coarse sand (cs), and conglomerate (cng). Not to scale horizontally.

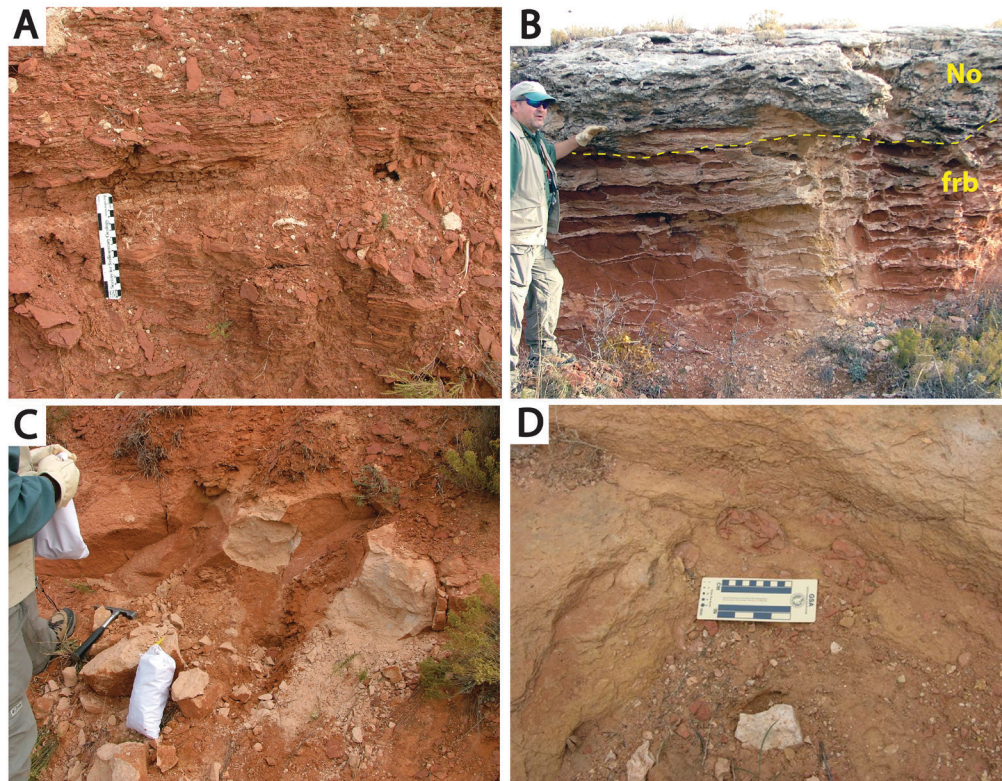


Figure 6. Field photos showing (A) fissile red beds facies in MS-4; (B) calcrete development at the unconformable contact in MS-2 between the Ogallala Formation (No) and the fissile red beds facies (frb); (C) the collection of the POR 4-1 sample for detrital zircon dating from a structureless sandstone interbedded with fissile siltstone facies; and (D) red mudstone rip-up clasts in a structureless sandstone bed near the base of MS-2.

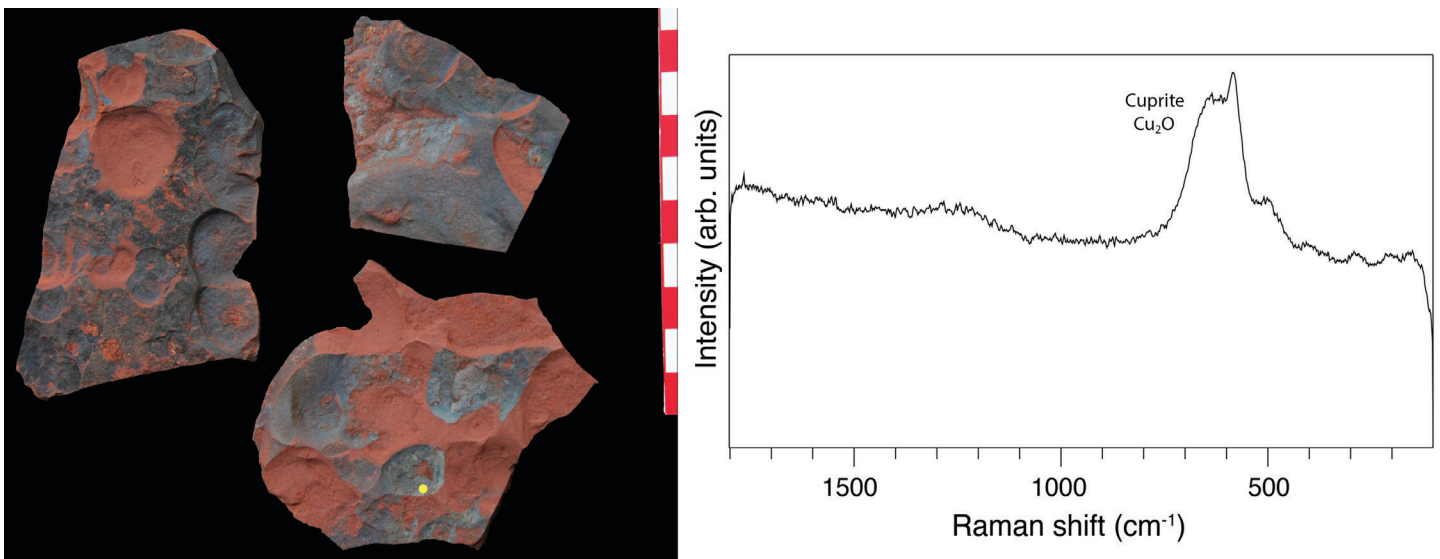


Figure 7. Red-bed siltstones from near MS-4 showing bluish varnish. Yellow dot shows where representative Raman spectra were collected. The spectrum shows two broad bands between 500 and 650  $\text{cm}^{-1}$ . These two distinctive broad bands are assigned to the triply degenerate Cu-O vibrational modes in the copper oxide lattice at 580 and 630  $\text{cm}^{-1}$ .

#### 4.1.4 Planar-laminated sandstone (figs. 8C–D)

Planar-laminated sandstone facies are thin to thick beds of very light gray (10YR 7/1), poorly cemented, very fine grained, well-sorted quartz grains (fig. 8C). This facies is characterized throughout by very thin, planar to slightly wavy, mud-draped laminae. The mud drapes are dark gray to very faint, depending on thickness, but are generally less than 1 mm thick (fig. 8D). As with the trough cross-bedded sandstone facies, nodular and sheet-like protrusions of calcareous cement stand in positive relief on some weathered surfaces.

#### 4.1.5 Mudstone clast conglomerate (fig. 8E)

The mudstone clast conglomerate facies is present in the MS-1 and MS-3 measured sections (fig. 5). The conglomerate is a 5–30 cm thick bed of clast- and matrix-supported clasts within an indurated, sandy mudstone matrix (fig. 8E). Composed of reddish-brown (2.5YR 5/4) mudrock and claystone chips with an unordered fabric, clasts range from 1 to 10 cm on their long axes. The upper and lower contacts are undulatory while the latter appears to scour into the underlying planar-laminated sandstone facies.

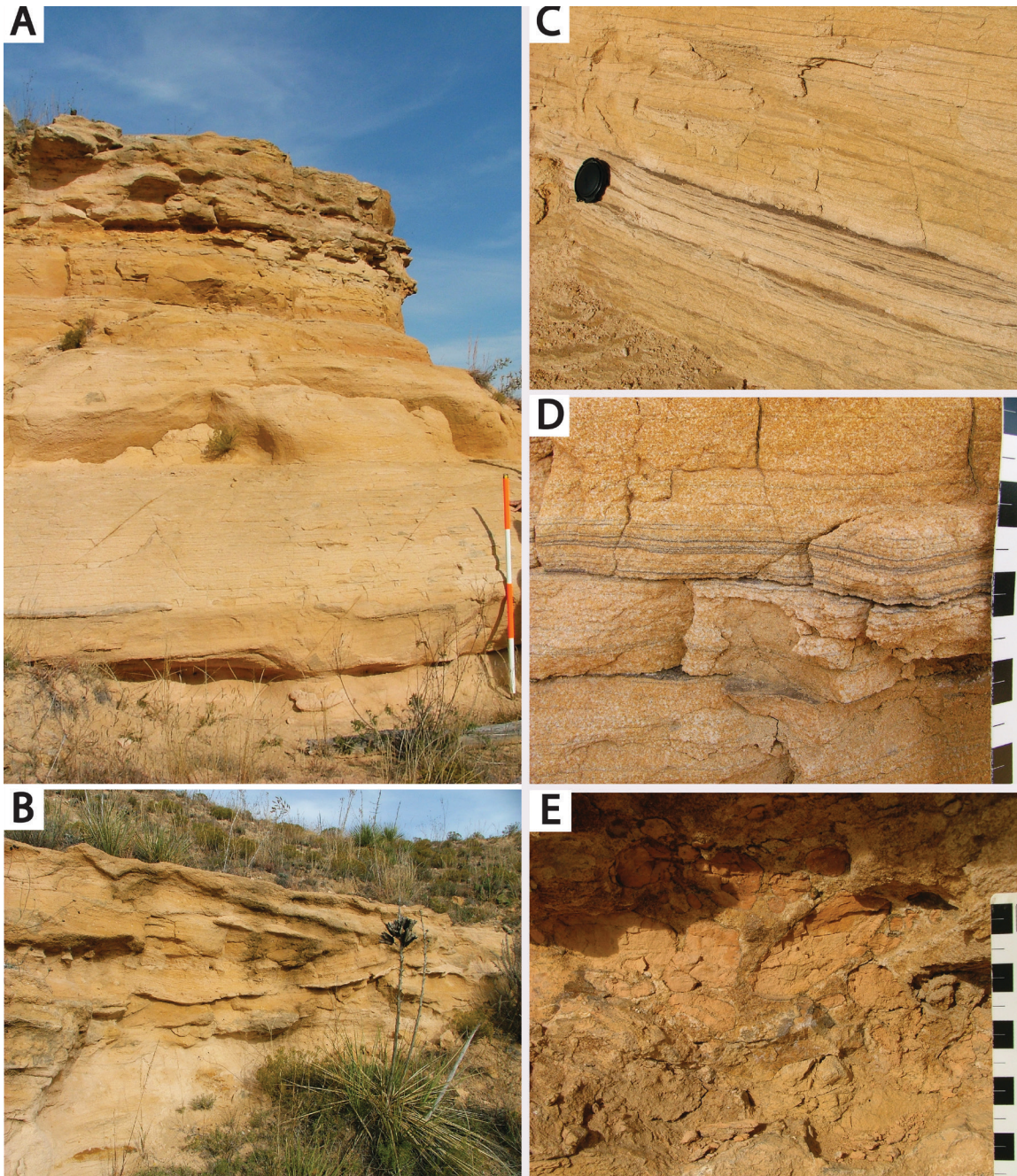


Figure 8. Field photos showing (A) 4.5 m of sandstone and conglomeratic deposits at the top of MS-1 (scale bar in 1-foot increments); (B) trough cross-bedded sandstone at the top of MS-3; (C) mud-draped laminae suggesting neap-spring tidal modulation in MS-1; (D) a close-up of the planar-laminated sandstone facies showing very thin mud drapes; and (E) red beds rip-up clasts of mudstone clast conglomerate facies.

## 4.2 Detrital zircon results

### 4.2.1 Age distributions and provenance

Detrital zircon age-probability plots for the three samples (fig. 9; raw DZ data included in Appendix 1) show a series of peaks or groups of peaks that define at least seven major zircon generating events on the North American continent (e.g., Dickinson and Gehrels, 2003, 2008, 2009; Soreghan and Soreghan, 2013). The oldest of these are Archean grains (more than 2,500 Ma) presumably from Laurentian cratons in the northern interior of the continent (fig. 10). Paleoproterozoic grains in North American strata are frequently associated with the Wopmay (2,300–1,800 Ma) and Yavapai-Mazatzal (1,800–1,535 Ma) orogens, though similar-aged zircons in Pennsylvanian rocks of the Appalachian Basin may have been derived from age-correlative events on the Gondwanan margin (Thomas et al., 2004). Mesoproterozoic grains are the most abundant DZ population (36.36% of all grains) and are attributed primarily to two sources: midcontinental anorogenic granites and rhyolites exposed during the Paleozoic in the Ancestral Rocky Mountains (1,535–1,300 Ma) and grains produced during the Grenville orogeny (1,300–905 Ma). Late Neoproterozoic grains are also abundant (32.52% of total) and are likely a mix of peri-Gondwanan terranes (750–510 Ma) uplifted and deposited along with Paleozoic zircons (510–285 Ma) during the Appalachian-Ouachita orogens along the east-southeastern margins of North America.

## 5. Discussion

### 5.1 Depositional interpretation

We interpret strata underlying the Ogallala Formation at Point of Rocks as overbank and tidally influenced fluvial deposits. The interbedded fissile red beds and structureless sandstone facies are interpreted as fine-grained overbank deposits (fig. 5, MS-2 and MS-4). Their general absence of primary sedimentary structures and red coloring suggest subaerial exposure and weak paleopedogenic modification. Structureless sandstones in these sections are interpreted as tabular sheet sands resulting from crevasse splays and rapid suspension deposition during floods. These units contain a higher fraction of clay- and silt-sized particles and are more erosive than the sandstones in the central measured sections. Copper oxides along parting laminations and fractures suggest that the exposed red beds once hosted copper sulfides. Copper-bearing sedimentary deposits, while rare in Jurassic or Cretaceous units, are abundant in both Permian and Triassic red-bed deposits in North America (Kirkham, 1989). In fact, some Permian red beds are an economically viable source of copper ore (Lambert et al., 1981). Copper-bearing minerals in Permian red beds include such sulfides as chalcocite ( $\text{Cu}_2\text{S}$ ) and chalcopyrite ( $\text{CuFeS}_2$ ) and carbonates such as malachite ( $\text{CuCO}_3\text{Cu}[\text{OH}]_2$ ) (e.g.,

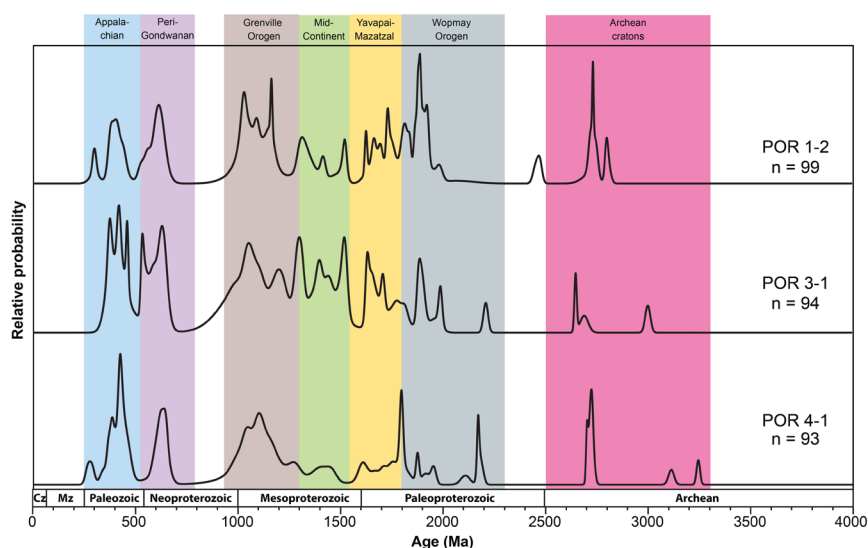


Figure 9. Age-distribution curves of detrital zircon ages from three bulk samples (POR 1-2, POR 3-1, and POR 4-1). Color swaths highlight seven significant igneous provinces and events (modified from Dickinson and Gehrels, 2009) that likely contributed to DZ populations of Point of Rocks samples; n = number of zircon grains sampled.

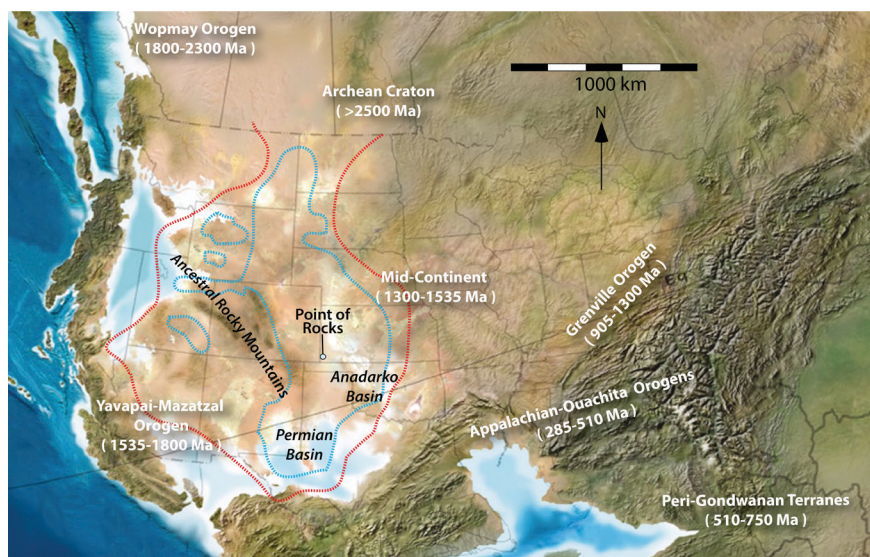


Figure 10. Paleogeographic map of North America for the Guadalupian series (~260 Ma; Blakey, 2013) showing distribution of Permian red beds (red dashed line) and evaporites (blue dashed lines) and the provinces and ages of basement rocks supplying detrital zircons to strata in North America (red bed and evaporite outlines modified from Walker, 1967; provenance data from Dickinson and Gehrels, 2009).

Johnson, 1974; Fay, 1975). Because sulfide minerals are unstable in oxidizing weathering environments, the cuprite likely formed as a product of recent weathering (fig. 7).

Resistant beds of trough cross-bedded sandstone crop out directly below the Point of Rocks and protrude southward from the bluff (fig. 5; MS-1 and MS-3). We interpret these sandstones to be fluvial and tidally influenced channel belt sandstones, incised into the red alluvial plain mudrocks. Tidal influences in the channel deposits are indicated by the thin mud drapes in planar-laminated

sandstones, which suggest tidal modulation and neap-spring cyclicity (fig. 8C–D). In modern river systems such as the Amazon, tidal currents induce up to m-scale changes in water level several hundred kilometers from the coast and influence flow as far as 800 km inland (Kvale and Archer, 2007). A prominent intraformational mud-chip conglomerate that contains red-bed clasts and scours into the probable tidal laminites is overlain by several meters of trough cross-bedded sandstones—apparently separating two stories in the channel. A structureless sandstone unit is also present within the channel fill (fig. 5, MS-1). Such structureless channel deposits may have resulted from bank collapse or liquefaction and flow of channel bars (Reading, 1996). In the lowermost channel sandstone unit, trough cross-beds indicating a southern paleoflow direction are well exposed in plain view.

### 5.2 Maximum depositional age

There are several methods for using the youngest uranium-lead ages of detrital zircons to constrain the maximum depositional age (MDA) of sedimentary units (Dickinson and Gehrels, 2010). One such method,  $YC2\sigma(3+)$ , is the weighted mean age of the youngest grouping of three or more grains overlapping in uranium-lead age at  $2\sigma$ . Based on the aggregated dataset of all three DZ samples, the mean age  $YC2\sigma(3+)$  of Point of Rocks strata is  $293 \pm 6.95$  Ma (fig. 11). Although  $YC2\sigma(3+)$  is a statistically robust measure of MDA, Dickinson and Gehrels (2010) in a study of Colorado Plateau sandstones with biostratigraphically controlled Mesozoic depositional ages found that  $YC2\sigma(3+)$  was also highly conservative and tended to be more than 10 m.y. older than accepted depositional age in the majority of cases. The youngest single grain (YSG) age at  $1\sigma$  in a DZ population, however, was found to be within the accepted age range of the deposit in more than 90% of the samples and within 5 million years of depositional age for 95% or more of the sandstones. The YSG age produced from Point of Rocks DZ grain samples is  $263.8 \pm 12.1$  Ma from sample POR 4-1. Significantly, both the YSG age and the conservative  $YC2\sigma(3+)$  suggest Permian maximum depositional ages.

Further refinement of maximum depositional age can be achieved through comparison of the Point of Rocks data with DZ age data from other late Paleozoic and Mesozoic units in the central and western United States (fig. 12). Detrital zircon ages of Point of Rocks strata show high degrees of overlap (0.89) and similarity (0.87) with such late Permian units as the Guadalupian Brushy Canyon and Bell Canyon Formations of the Delaware Mountain Group in the greater Permian Basin of New Mexico–West Texas (Soreghan and Soreghan, 2013). In comparison to the vertical succession

of Permian strata sampled from the Grand Canyon, the youngest Point of Rocks ages are most similar to the youngest 270–360 Ma peaks of the Permian Kaibab Formation (Gehrels et al., 2011). The youngest Point of Rocks DZ ages are also comparable to, though

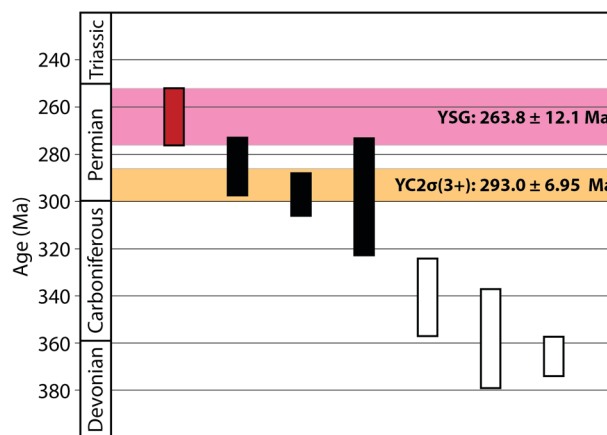


Figure 11. Maximum depositional ages calculated from the seven youngest uranium-lead ages at  $2\sigma$  (vertical bars) for the aggregated dataset of all Point of Rocks DZ ages. YSG: youngest single grain (red bar and pink stripe highlighting  $2\sigma$ );  $YC2\sigma(3+)$ : the weighted mean age of the three youngest overlapping detrital zircon ages at  $2\sigma$  (three black bars and orange stripe highlighting  $2\sigma$ ).

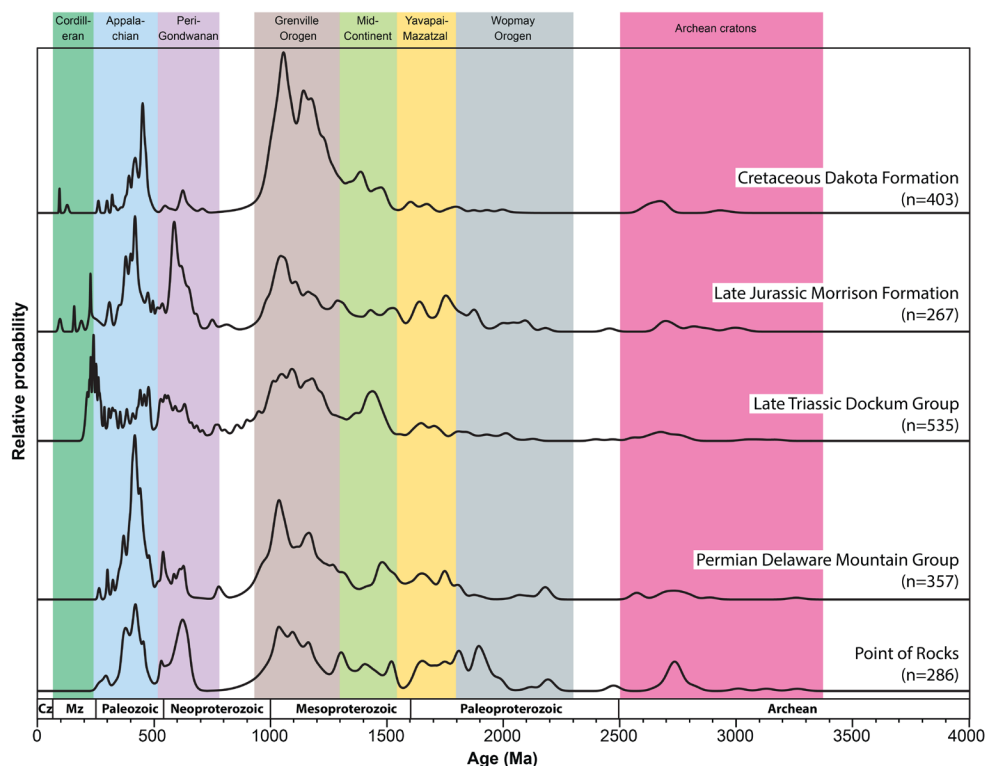


Figure 12. Normalized age-distribution curves of uranium-lead dates of detrital zircon from aggregated samples of Permian (Soreghan and Soreghan, 2013), Triassic (Dickinson and Gehrels, 2008), Jurassic (May et al., 2013), and Cretaceous (Finzel, 2014) formations and a composite of all zircon samples from the Point of Rocks;  $n$  = number of zircon grains analyzed.

younger than, the youngest 300–450 Ma population of DZ data from the middle Permian Flower-pot Shale and Blaine Formation of western Oklahoma (Sweet et al., 2013). These youngest DZ grains in Permian deposits were likely derived from Appalachian-Ouachita (285–510 Ma) orogenic sources along the east-southeastern margins of North America (fig. 10).

The youngest peaks of the Middle Triassic Moenkopi Formation, Chinle Formation, and Dockum Group, in contrast, are typically between ~200 and 285 Ma (Dickinson and Gehrels, 2008, 2010). Source areas for these youngest DZ populations likely included the Cordilleran magmatic arc (220–245 Ma) of western North America and the Ouachita foreland of Texas and northwest Mexico (Dickinson and Gehrels, 2009). Midcontinental Jurassic deposits such as the Sundance and Morrison Formations and the Cretaceous Dakota Formation typically exhibit young DZ ages in the 90–200 Ma range primarily from Cordilleran orogenic sources (Blum and Pecha, 2014; May et al., 2013; Finzel, 2014).

The similarity among the age spectra of all three DZ samples suggests that the episodes of deposition and incision occurred relatively rapidly, with no particularly extensive unconformities represented. Of course, a lag between zircon crystallization and deposition is common, which does not eliminate the possibility that the depositional age may be up to tens of millions of years younger than the youngest zircons (Gehrels et al., 2011). A lack of Mesozoic zircons in the red-bed and sandstone units exposed at Point of Rocks indicates a Permian maximum depositional age.

### 5.3 Paleogeographic considerations

Permian paleogeography on the North American midcontinent is in large part the story of shallow inland seas giving way to evaporite deposits and eolian environments following the assembly of Pangaea and a major global marine lowstand (fig. 10; West et al., 2010). At this time, the midcontinent was blanketed by sediments shed from the block-faulted Ancestral Rocky Mountains to the west and the Himalayan-sized Appalachian-Ouachita orogens to the east and southeast (Hatcher, 1987; Scotese and Langford, 1995). The area comprising modern Kansas was a complex patchwork of shallow marine and coastal environments on a broad ramp that sloped southward toward the Anadarko and Permian basins (West et al., 2010). Kansas was in an equatorial position during the Permian with a tropical to dry subtropical climate (Ziegler et al., 1998). By the late Permian, the shallow inland seas withdrew entirely to the south leaving extensive evaporite deposits and widespread eolian and fluvial red-bed landscapes (e.g., Benison and Goldstein, 2001; Zambito et al., 2012; Benison et al., 2013; Benison et al., 2015).

During the Triassic, midcontinent landscapes were erosional uplands and sedimentation had shifted west along the Chinle-Dockum paleodrainage systems of the Colorado Plateau and southern High Plains of Texas and New Mexico (Dickinson and Gehrels, 2008), so that no Triassic deposits are currently recognized in Kansas from outcrop or core (West et al., 2010). Though rocks of the Jurassic System were deposited over the western third of Kansas (Zeller, 1968), they are little studied because they are (as proposed in this study) encountered only in the subsurface. In Kansas, the Upper Jurassic Morrison Formation described from core is chiefly composed of gray to greenish-gray fine sandstones, siltstones, and calcareous mudrocks containing gypsum and anhydrite (Joeckel

et al., 2007). The vast majority of Mesozoic rocks in Kansas were deposited during the mid- to late Cretaceous Period while North America was again inundated by a large inland sea (Zeller, 1968). These rocks are mostly marine shales and carbonates, though the Cheyenne Sandstone and Dakota Formation at the base of the Cretaceous succession are predominantly fluvial sandstones and paleosols are common (Ludvigson et al., 2010; Retallack and Dilcher, 2012). Red beds are not reported from Jurassic or Cretaceous strata in Kansas.

Our interpretation of the depositional system at Point of Rocks is generally consistent with the Permian paleogeographic reconstructions in the midcontinent. Alluvial red-bed deposits are common in Permian strata throughout the region. Channel sandstones with north-south orientations and tidally influenced sedimentary structures are reasonable given the proximity of shallow seas to the south. Triassic rocks are seemingly missing entirely from Kansas, while Jurassic and Cretaceous strata in Kansas are lithologically distinct from rocks described at Point of Rocks.

### 5.4 Stratigraphic correlation

Assigning a geologic age to red beds at Point of Rocks has been complicated by the lack of observed fossils, a mix of previously unrecognized contrasting facies, and poor exposures. The DZ data presented here suggest correlation of these strata with one of the many red-bed successions in the Permian System. The uppermost Permian unit in Kansas is the Guadalupian Big Basin Formation (Zeller, 1968), referred to as the Taloga Formation in much of the older literature. The formation is characterized by red silty mudrocks and fine-grained red silty sandstones with some anhydrite and dolomite (West et al., 2010). O'Connor (1963) abandoned the name Taloga Formation in Kansas and reinstated the name Big Basin Formation used by Norton (1939) for all rocks between the Day Creek Dolomite and the top of the Permian unconformity. The Day Creek Dolomite is a fine-grained dolomite interbedded with red mudrocks and anhydrite and is mostly anhydrite at its thickest (~36 m) in the subsurface (Swineford, 1955). The Day Creek Dolomite is recognized as a reliable stratigraphic marker bed at the surface and in the subsurface (Norton, 1939). Norton (1939) reported approximately 19.8 m of Big Basin Formation (top of the Day Creek Dolomite to the base of the Cretaceous Kiowa Formation) in south-central Kansas and reported no fossils in the formation. Moore et al. (1951) noted that the maximum exposed thickness of the Big Basin Formation in Kansas was about 13.7 m at an outcrop area restricted to Clark and Meade counties east of Point of Rocks. Reported subsurface thicknesses range from ~48 m to more than 122 m (Edson, 1947; Merriam, 1963; Gutentag et al., 1981). Foster et al. (2014) identified the first magnetostratigraphic reversal of the Kiaman superchron (~267 Ma) in eolian deposits at the boundary between the middle Permian Dog Creek and Whitehorse Formations underlying the Day Creek Dolomite. These findings would support a maximum depositional age for the Big Basin Formation within the range of our YSG age ( $263.8 \pm 12.1$  Ma).

Red beds and sandstones were reported at shallow depths in three boreholes drilled within 5 km of the Point of Rocks study area (fig. 3 and fig. 13). The first was test hole 8 described by McLaughlin (1942). Note that the location reported for test hole 8 (NE sec. 12, T 34 S, R 43 W) places it in the uplands above the Ogallala outcrop to the east of Point of Rocks and about 30.5 m

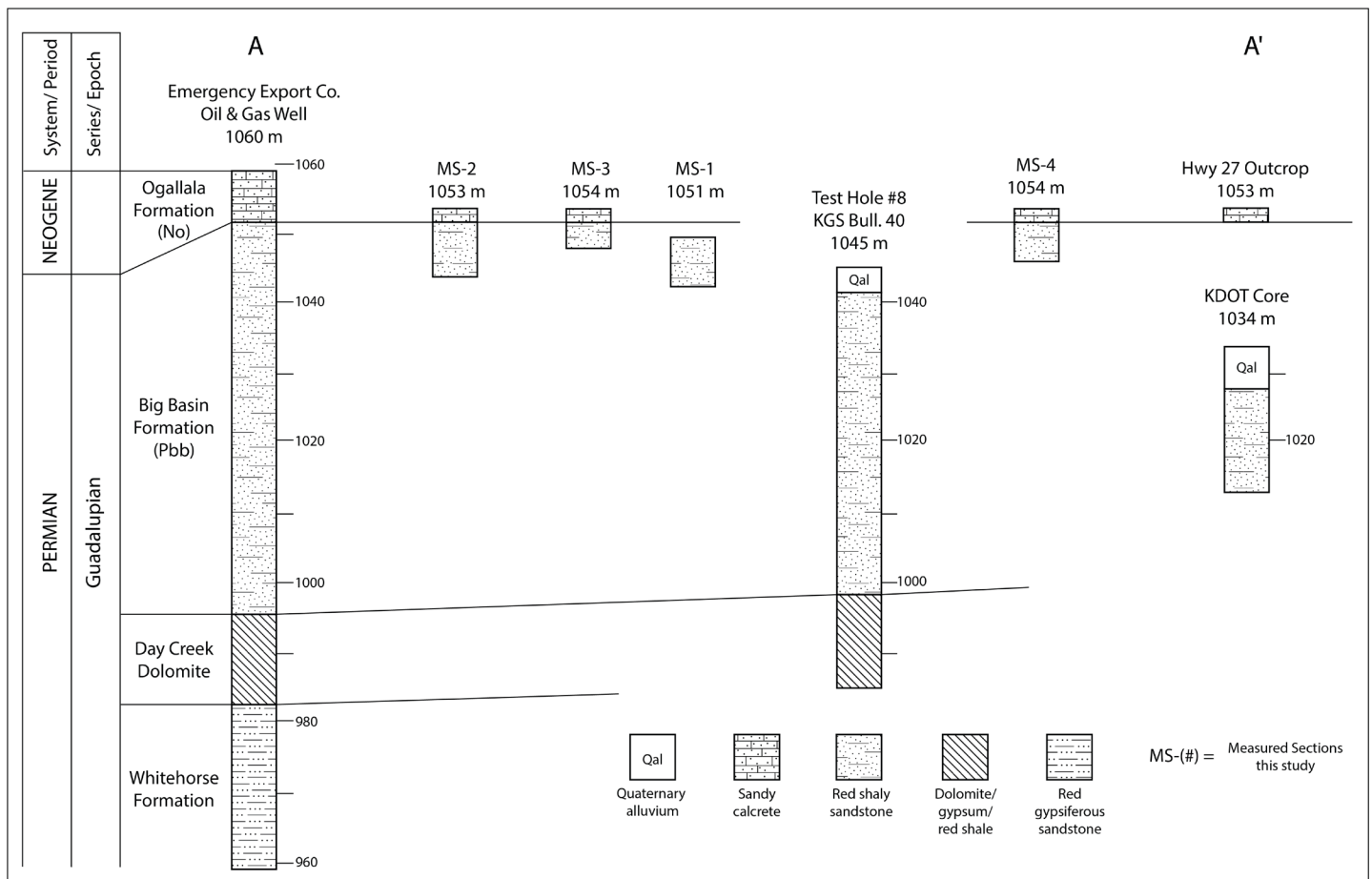


Figure 13. Composite cross section A–A' (fig. 2) showing measured sections (MS-1 to MS-4) and subsurface data from nearby tests (McLaughlin, 1942; Maher and Collins, 1952; and Croxton et al., 1998). Depths are marked in meters below sea level. Not to scale horizontally.

higher than the reported elevation. Based on the reported elevation (1,044.7 m) and the amount of alluvium logged (3.6 m), the correct location of test hole 8 is probably NE SE sec. 12 in the floodplain at the base of the exposure. There, McLaughlin (1942) reported interbedded red sandstone and siltstone to a depth of ~47 m underlain by ~14 m of maroon siltstone and gypsum to the bottom (61 m) of the hole. The second borehole was an Emergency Export Co. oil and gas test approximately 1.46 km northwest of Point of Rocks (Maher and Collins, 1952). Logs for that hole show red shaly sandstone from the base of the Ogallala unconformity to a depth of ~66 m underlain by ~14 m of dolomite, reddish-brown shale, and anhydrite. The third was a 20-m borehole drilled by the Kansas Department of Transportation (KDOT) approximately 4.2 km northeast of Point of Rocks along Kansas Highway 27. Logs for that hole showed ~15 m of red shaly sandstone below ~5 m of Cimarron River alluvium (Croxton et al., 1998).

The ~14 m thick gypsum- or anhydrite-rich, dolomitic, shaly unit encountered in the Emergency Export Co. oil and gas test (Maher and Collins, 1952) and test hole 8 (see Sawin, 2015) have been interpreted as the regional Day Creek Dolomite marker bed (fig. 13). Thus, we assign overlying red-bed units observed in drillers' logs and the outcrop at Point of Rocks to the Guadalupian Big Basin Formation. This interpretation is consistent with the subsurface data and the detrital zircon data collected from the measured sections.

## 6. Conclusions

Uranium-lead dating of detrital zircons was applied to samples of exposed non-fossiliferous strata underlying the Ogallala Formation at Point of Rocks in Morton County, Kansas, to better constrain the depositional age of the rocks. Red beds composed of fissile shale and sandstone are interpreted as alluvial overbank deposits, while dominantly trough cross-bedded and planar-laminated sandstones are interpreted as tidally influenced fluvial channel deposits. The channel sandstones are better cemented and more resistant to weathering than the red beds and defended the overlying escarpment of the Ogallala Formation from erosional retreat along the north bluff line of the Cimarron River valley.

Age spectra of the DZ samples from the site can be grouped into at least seven subpopulations with a youngest single zircon age of  $263.8 \pm 12.1$  Ma and a more conservative  $YC2\sigma(3+)$  age of  $293.0 \pm 6.95$  Ma. These ages suggest that the red beds were deposited in the Permian. Comparisons to DZ age spectra from other Permian units in western North America and a lack of Mesozoic-aged zircons support this interpretation. Copper oxides along partings and fractures suggest that Point of Rocks once hosted copper sulfides. Copper sulfides are common in regional Permian-Triassic red beds. We reject previous interpretations of Triassic, Jurassic, or Cretaceous ages for the red-bed strata at Point of Rocks. The DZ data, in conjunction with the likely identification of the Day

Creek Dolomite marker bed in logs of nearby drilling operations, strongly suggest that the enigmatic strata cropping out at the base of Point of Rocks are Permian red beds of the Guadalupian Big Basin Formation.

### Acknowledgments

The authors thank Dr. George Gehrels and Roswell Juan of the Arizona LaserChron Center. We also thank District Ranger Joe Hartman and USDA Forest Service staff at the Cimarron National Grassland. We thank Drs. Kathleen Benison and Michael Blum for their technical reviews and thoughtful critiques of the manuscript. Cathy Evans (KGS) improved the clarity of the manuscript and for that we are grateful, and we thank Julie Tollefson (KGS) for editorial handling and publication assistance.

### Notes

1 In 1968, the KGS published *The Stratigraphic Succession in Kansas* (Zeller, 1968), which brought together for the first time the nomenclature, description of geologic units, and a graphic presentation on one chart (Plate 1) of the classification of rocks in Kansas. Zeller (1968) is nearly 50 years old and is in the process of being revised by the KGS. However, until revisions are published, it remains the most recent accepted stratigraphic guide and chart for Kansas.

### References

- Benison, K. C., and Goldstein, R. H., 2001, Evaporites and siliciclastics of the Permian Nippewalla Group, Kansas and Oklahoma: A case for nonmarine deposition: *Sedimentology*, v. 48, p. 165–188.
- Benison, K. C., Zambito, J. J., and Knapp, J. P., 2015, Contrasting siliciclastic-evaporite strata in subsurface and outcrop: An example from the Permian Nippewalla Group of Kansas, U.S.A.: *Journal of Sedimentary Research*, v. 85, p. 626–645.
- Benison, K. C., Zambito, J. J., Soreghan, G. S., Soreghan, M. J., Foster, T. M., and Kane, M. J., 2013, Permian red beds and evaporites of the Amoco Rebecca K. Bounds core, Greeley County, Kansas: Implications for science and industry; *in*, Midcontinent core workshop: From source to reservoir to seal, Midcontinent Section American Association of Petroleum Geologists, M. K. Dubois, W. L. Watney, and J. Tollefson, eds.: Midcontinent Core Workshop: From Source to Reservoir to Seal, Midcontinent Section American Association of Petroleum Geologists, Kansas Geological Survey and Kansas Geological Society, Wichita, Kansas, p. 9–14.
- Blakey, R. C., 2013, Paleogeographic and tectonic history of North America—Key time slices: Colorado Plateau Geosystems, Inc., <http://cpgeosystems.com/namkeypaleogeography.html> (accessed August 15, 2015).
- Blum, M., and Pecha, M., 2014, Mid-Cretaceous to Paleocene North American drainage reorganization from detrital zircons: *Geology*, v. 42, no. 7, p. 607–610.
- Croxton, N. M., Geist, J. W., and Peterson, A. E., 1998, Bridge foundation geology report, K-27 over the Cimarron River, Morton County, Kansas: Kansas Department of Transportation, Topeka, Kansas, 9 p.
- Dickinson, W. R., and Gehrels, G. E., 2003, U-Pb ages of detrital zircons from Permian and Jurassic eolian sandstones of the Colorado Plateau, USA: Paleogeographic implications: *Sedimentary Geology*, v. 163, p. 29–66.
- Dickinson, W. R., and Gehrels, G. E., 2008, U-Pb ages of detrital zircons in relation to paleogeography: Triassic paleodrainage networks and sediment dispersal across southwest Laurentia: *Journal of Sedimentary Research*, v. 78, p. 745–764.
- Dickinson, W. R., and Gehrels, G. E., 2009, Use of U-Pb ages of detrital zircons to infer maximum depositional ages of strata: A test against a Colorado Plateau Mesozoic database: *Earth and Planetary Science Letters*, v. 288, p. 115–125.
- Dickinson, W. R., and Gehrels, G. E., 2010, Insights into North American paleogeography and paleotectonics from U-Pb ages of detrital zircons in Mesozoic strata of the Colorado Plateau, USA: *International Journal of Earth Sciences*, v. 99, p. 1,247–1,265.
- Dickinson, W. R., Gehrels, G. E., and Marzolf, J. E., 2010, Detrital zircons from fluvial Jurassic strata of the Michigan basin: Implications for the transcontinental Jurassic paleoriver hypothesis: *Geology*, v. 38, p. 499–502.
- Edson, F. C., 1947, Subsurface geologic cross section from Ford County, Kansas, to Dallam County, Texas: Kansas Geological Survey, Oil and Gas Investigations, Preliminary Cross Section No. 3.
- Fay, R. O., 1975, A possible origin for copper in Oklahoma: *Oklahoma Geology Notes*, v. 35, no. 4, p. 151–153.
- Finzel, E. S., 2014, Detrital zircons from Cretaceous midcontinent strata reveal an Appalachian Mountains–Cordilleran foreland basin connection: *Lithosphere*, v. 6, no. 5, p. 378–382.
- Foster, T., Soreghan, G. S., Soreghan, M. J., Benison, K. C., and Elmore, R. D., 2014, Climatic and paleogeographic significance of aeolian sediment in the middle Permian Dog Creek Shale (Midcontinent U.S.): *Palaeogeography, Palaeoclimatology, Palaeoecology*, v. 402, p. 12–29.
- Gehrels, G. E., 2012, Detrital zircon U-Pb geochronology: Current methods and new opportunities; *in*, *Tectonics of sedimentary basins: Recent advances*, C. Busby and A. A. Perez, eds.: Hoboken, New Jersey, Wiley-Blackwell, p. 47–62.
- Gehrels, G. E., Blakey, R., Karlstrom, K. E., Timmons, J. M., Dickinson, B., and Pecha, M., 2011, Detrital zircon U-Pb geochronology of Paleozoic strata in the Grand Canyon, Arizona: *Lithosphere*, v. 3, p. 183–200.
- Gehrels, G. E., Valencia, V., and Pullen, A., 2006, Detrital zircon geochronology by laser-ablation multicollector ICPMS at the Arizona LaserChron Center; *in*, *Geochronology: Emerging opportunities*, Paleontology Society short course, T. Loszewski and W. Huff, eds.: Paleontology Society Papers, v. 11, 10 p.
- Gehrels, G. E., Valencia, V., and Ruiz, J., 2008, Enhanced precision, accuracy, efficiency, and spatial resolution of U-Pb ages by laser ablation–multicollector–inductively coupled plasma–mass spectrometry: *Geochemistry Geophysics Geosystems*, v. 9, Q03017, doi:10.1029/2007GC001805.
- Gould, C. N., 1901, The Dakota Cretaceous of Kansas and Nebraska: *Kansas Academy of Science Transactions*, v. 17, p. 122–178.
- Gutentag, E. D., Lobmeyer, D. H., and Slagle, S. E., 1981, Geohydrology of southwestern Kansas: Kansas Geological Survey, Irrigation Series 7, 73 p.
- Hatcher, R. D., Jr. 1987, Tectonics of the southern and central Appalachian intermides: *Annual Review of Earth and Planetary Sciences*, v. 15, p. 337–362.
- Joeckel, R. M., Ludvigson, G. A., Wally, K. D., and Doveton, J. H., 2007, Preliminary analysis of the Upper Jurassic Morrison Formation in the Rebecca Bounds Core, western Kansas: *Geological Society of America Abstracts with Programs*, v. 39, no. 6, p. 338.
- Johnson, K. S., 1974, Permian copper shales of Southwestern United States; *in*, *Gisements stratiformes et provinces cuprifères*, P. Bartholomé, ed.: Société Géologique de Belgique, p. 383–393.
- Johnson, W. C., Woodburn, T. L., and Messinger, L. G., 2009, Surficial geology of Morton County, Kansas: Kansas Geological Survey, Map M-116, 1 sheet, 47 x 38 inches, scale 1:50,000.
- Kansas Geological Survey, 1991, Geologic Map of Kansas: Kansas Geological Survey, Map M-23, 1:500,000 scale.
- Kirkham, R. V., 1989, Distribution, settings, and genesis of sediment-

- hosted stratiform copper deposits; *in*, Sediment-hosted stratiform copper deposits, R. W. Boyle, A. C. Brown, C. W. Jefferson, E. C. Jowett, and R. V. Kirkham, eds.: Geological Association of Canada Special Paper 36, p. 3–38.
- Kume, J., and Spinazola, J. M., 1985, Geohydrology of sandstone aquifers in southwestern Kansas: Kansas Geological Survey, Irrigation Series 8, 49 p.
- Kvale, E. P., and Archer, A. W., 2007, Paleovalley fills—Trunk vs. tributary: American Association of Petroleum Geologists, Bulletin, v. 91, no. 6, p. 809–821.
- Lambert, M. W., Berenden, P., and Ripley, E. M., 1981, Copper sulfides in the Lower Permian redbeds of south-central Kansas: Kansas Geological Survey, Bulletin 223, part 2, [http://www.kgs.ku.edu/Publications/Bulletins/223\\_2/index.html](http://www.kgs.ku.edu/Publications/Bulletins/223_2/index.html).
- Liggett, G. A., and Zakrzewski, R. J., 1997 (revised 1998), Final report on the geological and paleontologic investigation of the Cimarron National Grassland: Fort Hays State University and U.S. Department of Agriculture Forest Service contract #CC2-2-12-94-07-028, 29 p.
- Liggett, G. A., Zakrzewski, R. J., and McNinch, K. L., 1998, Geologic and paleontologic investigation of the Cimarron National Grassland, Morton County, Kansas: *Dakoterra*, v. 5, p. 123–126.
- Ludvigson, G. A., Witzke, B. J., Joeckel, R. M., Ravn, R. L., Phillips, P. L., González, L. A., and Brenner, R. L., 2010, New insights on the sequence stratigraphic architecture of the Dakota Formation in Kansas–Nebraska–Iowa from a decade of sponsored research activity: Kansas Geological Survey, Current Research in Earth Sciences, Bulletin 258, part 2, <http://www.kgs.ku.edu/Current/2010/Ludvigson/index.html>.
- Ludwig, K. R., 2012, Isoplot 3.75: A geochronological toolkit for Microsoft Excel: Berkeley Geochronology Center Special Publication No. 5, revised January 30, 2012.
- Maher, J. C., and Collins, J. B., 1952, Correlation of Permian and Pennsylvanian rocks of western Kansas to the Front Range of Colorado: U.S. Geological Survey, Oil and Gas Investigations, Chart OC-46, 3 sheets.
- May, S. R., Gray, G. G., Summa, L. L., Stewart, N. R., Gehrels, G. E., and Pecha, M. E., 2013, Detrital zircon geochronology from the Bighorn Basin, Wyoming, USA: Implications for tectonostratigraphic evolution and paleogeography: Geological Society of America Bulletin, v. 125, p. 1,403–1,422.
- McLaughlin, T. G., 1942, Geology and ground-water resources of Morton County, Kansas: Kansas Geological Survey, Bulletin 40, 126 p.
- McNinch, K. L., 1996, An integrated GIS database, geologic and paleontologic reconnaissance, and areal correlation of soils to geology within Cimarron National Grasslands (sic), Morton County, Kansas: M.S., Fort Hays State University, 99 p.
- Merriam, D. F., 1963, The geologic history of Kansas: Kansas Geological Survey, Bulletin 162, 317 p.
- Moore, R. C., Frye, J. C., and Jewett, J. M., 1944, Tabular description of outcropping rocks in Kansas: Kansas Geological Survey, Bulletin 52, part 4, p. 137–212.
- Moore, R. C., Frye, J. C., Jewett, J. M., Lee, W., and O'Connor, H. G., 1951, The Kansas rock column: Kansas Geological Survey, Bulletin 89, 132 p.
- Moore, R. C., Frye, J. C., Jewett, J. M., Lee, W., and O'Connor, H. G., 1952, Graphic column of Kansas rocks: Kansas Geological Survey, 1 sheet.
- Moore, R. C., and Landes, K. K., 1937, Geologic map of Kansas: Kansas Geological Survey, scale 1:500,000.
- Munsell Color, 2000, Munsell Soil Color Chart, Baltimore, Maryland, 22 p.
- Norton, G. H., 1939, Permian redbeds in Kansas: American Association of Petroleum Geologists, Bulletin, v. 23, no. 12, p. 1,751–1,815.
- O'Connor, H. G., 1963, Changes in Kansas stratigraphic nomenclature: American Association of Petroleum Geologists, Bulletin, v. 47, no. 10, p. 1,873–1,877.
- Reading, H. G., 1996, Sedimentary environments: Processes, facies and stratigraphy, 3<sup>rd</sup> edition. Oxford, Blackwell Science, 688 p.
- Retallack, G. J., and Dilcher, D. L., 2012, Outcrop versus core and geophysical log interpretation of mid-Cretaceous paleosols from the Dakota Formation of Kansas: *Palaeogeography, Palaeoclimatology, Palaeoecology*, v. 329, p. 47–63.
- Sawin, R. S., 2015, Copies of archived correspondence pertinent to the decision to classify the exposure at Point of Rocks, Morton County, Kansas, as Jurassic by the Kansas Geological Survey in 1967: Kansas Geological Survey, Open-File Report 2015-2, 11 p.
- Scotese, C. R., and Langford, R. P., 1995, Pangea and the paleogeography of the Permian; *in*, The Permian of Northern Pangea, vol. 1, P. A. Scholle, T. M. Peryt, and D. S. Ilmer-Scholle, eds.: Berlin, Springer-Verlag, p. 3–19.
- Smith, H. T. U., 1940, Geological studies in southwestern Kansas: Kansas Geological Survey, Bulletin 34, 212 p.
- Soreghan, G. S., and Soreghan, M. J., 2013, Tracing clastic delivery to the Permian Delaware Basin, USA: Implications for paleogeography and circulation in westernmost equatorial Pangea: *Journal of Sedimentary Research*, v. 83, p. 786–802.
- Sweet, A. C., Soreghan, G. S., Sweet, D. E., Soreghan, M. J., and Madden, A. S., 2013, Permian dust in Oklahoma: Source and origin for Middle Permian (Flowerpot-Blaine) redbeds in western tropical Pangea: *Sedimentary Geology*, v. 284–285, p. 181–196.
- Swineford, A., 1955, Petrography of Upper Permian rocks in south-central Kansas: Kansas Geological Survey, Bulletin 111, 179 p.
- Thomas, W. A., Becker, T. P., Samson, S. D., and Hamilton, M. A., 2004, Detrital zircon evidence of a recycled orogenic foreland provenance for Alleghenian clastic-wedge sandstones: *Journal of Geology*, v. 112, p. 23–37.
- Walker, T. R., 1967, Formation of red beds in modern and ancient deserts: *Bulletin of the Geological Society of America*, v. 78, p. 353–368.
- West, R. R., Miller, K. B., and Watney, W. L., 2010, The Permian System in Kansas: Kansas Geological Survey, Bulletin 257, 82 p.
- Williams, P. F., and Porto, S. P. S., 1973, Symmetry-forbidden resonant Raman scattering in Cu<sub>2</sub>O: *Physical Review B* 4, p. 1,782–1,785.
- Zambito, J. J., Benison, K. C., Foster, T., Soreghan, G. S., Kane, M., and Soreghan, M. J., 2012, Lithostratigraphy of the Permian red beds and evaporites in the Rebecca K. Bounds, Core, Greeley County, Kansas: Kansas Geological Survey, Open-File Report 2012-15, 45 p.
- Zeller, D. E., ed., 1968, The stratigraphic succession in Kansas: Kansas Geological Survey, Bulletin 189, 81 p., 1 plate, <http://www.kgs.ku.edu/Publications/Bulletins/189/index.html>.
- Ziegler, A. M., Gibbs, M. T., and Hulver, M. L., 1998, A mini-atlas of oceanic water masses in the Permian Period: *Proceedings of the Royal Society of Victoria*, v. 110, no. 1/2, p. 323–343.

Appendix 1. Table 1. POR1-2 U-Pb geochronologic analyses.

Analysis	Isotope ratios										Apparent ages (Ma)						Best age (Ma)	Conc (%)	
	U (ppm)	206Pb/204Pb	U/Th	206Pb* ± (%)	207Pb* ± (%)	206Pb* ± (%)	207Pb* ± (%)	error corr.	206Pb* ± (%)	235U*	207Pb* ± (%)	206Pb* ± (%)	207Pb* ± (%)	± (Ma)	± (Ma)	± (Ma)			
POR1-2-4	137	3839	0.9	18.6657	15.8	0.3480	16.1	0.0471	3.1	0.19	296.8	9.0	303.2	42.2	353.2	296.8	9.0	NA	
POR1-2-78	773	1715	0.6	17.5510	4.5	0.3712	9.7	0.0473	8.5	0.88	297.6	24.8	320.5	26.6	490.6	99.8	297.6	24.8	NA
POR1-2-73	112	10332	1.0	18.2987	9.0	0.4489	9.7	0.0596	3.7	0.38	373.0	13.4	376.5	30.6	397.9	202.1	373.0	13.4	NA
POR1-2-8	754	6184	39.2	17.8793	2.7	0.4621	4.2	0.0599	3.1	0.75	375.2	11.4	385.7	13.3	449.6	60.7	375.2	11.4	NA
POR1-2-63	225	37556	2.6	18.0318	6.4	0.4803	7.3	0.0628	3.7	0.50	392.7	13.9	398.3	24.2	430.7	141.7	392.7	13.9	NA
POR1-2-5	493	2394	3.0	17.6539	3.4	0.4994	6.1	0.0639	5.1	0.84	399.5	19.8	411.3	20.7	477.7	74.3	399.5	19.8	NA
POR1-2-54	53	5977	2.4	18.5763	24.7	0.4810	26.1	0.0648	8.4	0.32	404.8	33.1	398.8	86.2	364.0	564.0	404.8	33.1	NA
POR1-2-49	193	30889	5.3	18.1014	6.1	0.4954	6.8	0.0650	3.2	0.47	406.2	12.5	408.6	23.0	422.1	135.3	406.2	12.5	NA
POR1-2-7	130	39051	1.6	16.7893	4.3	0.5491	5.9	0.0669	4.2	0.70	417.2	16.8	444.4	21.4	587.7	92.4	417.2	16.8	71.0
POR1-2-87	364	56798	1.1	17.9709	2.3	0.5415	3.9	0.0706	3.1	0.81	439.7	13.3	439.4	13.8	438.2	50.9	439.7	13.3	NA
POR1-2-43	67	15379	0.7	17.8339	15.4	0.5542	16.8	0.0717	6.8	0.40	446.3	29.3	447.8	61.0	455.3	343.4	446.3	29.3	NA
POR1-2-80	177	53419	2.3	17.1622	2.0	0.6785	3.6	0.0845	2.9	0.83	522.6	14.8	525.9	14.6	539.9	43.5	522.6	14.8	96.8
POR1-2-20	84	51272	1.2	16.5121	7.7	0.7510	8.5	0.0899	3.7	0.44	555.1	19.8	568.8	37.2	623.3	166.0	555.1	19.8	89.0
POR1-2-42	221	47071	1.4	16.8689	2.7	0.7366	3.9	0.0901	2.7	0.70	556.2	14.5	560.4	16.6	577.4	59.7	556.2	14.5	96.3
POR1-2-72	158	56217	0.7	16.7338	4.9	0.7914	5.7	0.0960	2.8	0.50	591.2	16.0	592.0	25.5	594.9	106.8	591.2	16.0	99.4
POR1-2-13	339	241722	5.9	16.2539	1.1	0.8300	2.9	0.0978	2.7	0.93	601.7	15.5	613.6	13.4	657.6	23.5	601.7	15.5	91.5
POR1-2-23	370	98816	1.3	16.2738	1.9	0.8375	5.3	0.0988	5.0	0.94	607.6	29.1	617.7	24.7	654.9	40.0	607.6	29.1	92.8
POR1-2-102	76	19445	1.1	16.3932	7.8	0.8319	8.5	0.0989	3.5	0.41	608.0	20.4	614.6	39.3	639.3	167.1	608.0	20.4	95.1
POR1-2-59	48	11427	1.2	15.9301	10.0	0.8696	11.7	0.1005	6.1	0.52	617.1	36.0	635.3	55.3	700.6	212.9	617.1	36.0	88.1
POR1-2-67	237	107522	1.1	16.4351	1.8	0.8460	3.4	0.1008	2.8	0.84	619.3	16.8	622.4	15.8	633.8	39.8	619.3	16.8	97.7
POR1-2-34	55	12517	1.7	15.7126	9.7	0.8969	10.2	0.1022	3.2	0.32	627.3	19.3	650.0	49.0	729.8	205.6	627.3	19.3	86.0
POR1-2-83	486	63653	0.9	16.5753	0.6	0.8557	4.8	0.1029	4.8	0.99	631.2	28.9	627.8	22.7	615.4	13.6	631.2	28.9	102.6
POR1-2-85	278	65455	2.8	16.5406	4.0	0.8576	5.5	0.1029	3.8	0.69	631.3	22.9	628.8	25.9	620.0	86.2	631.3	22.9	101.8
POR1-2-70	79	32111	3.4	13.8980	3.4	1.7118	4.2	0.1725	2.4	0.58	1026.1	23.1	1013.0	26.9	984.6	69.5	984.6	69.5	104.2
POR1-2-39	243	14050	2.5	13.7271	1.8	1.6601	4.2	0.1653	3.8	0.91	986.1	34.6	993.4	26.5	1009.7	36.0	1009.7	36.0	97.7
POR1-2-28	100	80776	3.4	13.7057	3.4	1.7280	5.2	0.1718	4.0	0.77	1021.8	38.0	1019.0	33.7	1012.9	68.1	1012.9	68.1	100.9
POR1-2-36	291	206802	3.4	13.6745	0.8	1.7279	3.8	0.1714	3.7	0.98	1019.6	35.0	1019.0	24.4	1017.5	16.0	1017.5	16.0	100.2
POR1-2-48	293	112824	30.8	13.6102	1.6	1.6866	2.2	0.1665	1.6	0.70	992.7	14.4	1003.5	14.3	1027.0	32.6	1027.0	32.6	96.7
POR1-2-41	761	169226	58.8	13.6098	0.5	1.7957	3.0	0.1772	3.0	0.99	1051.9	28.7	1043.9	19.6	1027.1	10.2	1027.1	10.2	102.4
POR1-2-55	168	131862	2.4	13.5669	1.9	1.8152	3.2	0.1786	2.6	0.81	1059.4	25.1	1051.0	20.8	1033.5	38.1	1033.5	38.1	102.5
POR1-2-61	318	155882	0.8	13.5616	0.8	1.8515	3.2	0.1821	3.1	0.97	1078.5	31.1	1063.9	21.4	1034.3	17.1	1034.3	17.1	104.3
POR1-2-37	218	87780	2.3	13.4446	1.2	1.8593	3.0	0.1813	2.8	0.92	1074.1	27.8	1066.8	20.0	1051.8	23.3	1051.8	23.3	102.1
POR1-2-88	46	23089	1.0	13.4226	4.4	1.8853	7.6	0.1835	6.2	0.82	1086.3	62.1	1075.9	50.5	1055.1	88.1	1055.1	88.1	103.0
POR1-2-66	184	154633	3.8	13.3800	1.1	1.8450	3.4	0.1790	3.2	0.94	1061.7	31.4	1061.6	22.4	1061.5	22.8	1061.5	22.8	100.0
POR1-2-26	97	77991	2.1	13.3778	2.7	1.8887	6.1	0.1833	5.5	0.90	1084.7	54.7	1077.1	40.5	1061.8	53.6	1061.8	53.6	102.2
POR1-2-81	69	62105	0.9	13.3764	3.7	1.8165	5.9	0.1762	4.6	0.78	1046.3	44.8	1051.4	38.8	1062.0	74.3	1062.0	74.3	98.5
POR1-2-21	625	318815	6.8	13.1863	0.6	1.9330	3.1	0.1849	3.1	0.98	1093.5	30.9	1092.6	20.9	1090.7	11.4	1090.7	11.4	100.3
POR1-2-95	95	48457	2.4	13.1349	1.4	1.9501	3.8	0.1858	3.5	0.93	1098.4	35.7	1098.5	25.6	1098.6	28.6	1098.6	28.6	100.0
POR1-2-93	260	91958	6.1	13.0984	1.4	2.1731	4.5	0.2064	4.3	0.95	1209.8	47.3	1172.5	31.4	1104.1	28.1	1104.1	28.1	109.6
POR1-2-3	226	192592	4.0	12.9044	1.3	2.0365	3.4	0.1906	3.2	0.93	1124.6	33.0	1127.8	23.4	1133.9	25.4	1133.9	25.4	99.2
POR1-2-90	161	1994	2.7	12.8850	3.0	1.5439	6.5	0.1443	5.7	0.88	868.8	46.4	948.1	39.8	1136.9	60.0	1136.9	60.0	76.4
POR1-2-99	173	62387	5.6	12.7864	1.5	2.1850	10.3	0.2026	10.2	0.99	1189.4	110.7	1176.3	71.9	1152.1	30.3	1152.1	30.3	103.2
POR1-2-35	211	141692	2.4	12.7512	0.8	2.1080	2.4	0.1948	2.2	0.93	1147.1	23.2	1150.8	16.3	1157.6	16.7	1157.6	16.7	99.2
POR1-2-65	466	81796	2.9	12.7211	0.2	2.0752	1.1	0.1915	1.0	0.98	1129.3	10.9	1140.6	7.3	1162.3	4.4	1162.3	4.4	97.1
POR1-2-44	189	69030	1.8	12.7196	1.2	2.2527	6.8	0.2078	6.7	0.99	1217.2	74.1	1197.6	47.7	1162.5	23.1	1162.5	23.1	104.7
POR1-2-46	148	90579	3.7	12.7133	2.1	2.0770	4.6	0.1915	4.1	0.90	1129.6	43.0	1141.3	31.7	1163.5	40.7	1163.5	40.7	97.1
POR1-2-57	51	43914	3.3	12.2897	3.8	2.3173	5.2	0.2065	3.5	0.68	1210.4	39.1	1217.6	36.8	1230.4	74.5	1230.4	74.5	98.4
POR1-2-74	94	47840	3.5	11.8994	2.4	2.5136	6.8	0.2169	6.4	0.94	1265.6	73.2	1276.0	49.5	1293.4	46.8	1293.4	46.8	97.9
POR1-2-45	170	120689	0.9	11.8465	0.7	2.6636	3.4	0.2289	3.3	0.98	1328.5	40.0	1318.4	25.2	1302.1	14.5	1302.1	14.5	102.0
POR1-2-76	109	90953	3.5	11.8144	1.2	2.6940	4.1	0.2308	3.9	0.96	1338.9	47.3	1326.8	30.3	1307.3	23.3	1307.3	23.3	102.4
POR1-2-10	283	245857	3.5	11.7198	0.9	2.6106	2.6	0.2219	2.5	0.94	1291.9	29.2	1303.6	19.5	1322.9	17.2	1322.9	17.2	97.7
POR1-2-82	119	121863	3.0	11.5808	1.1	2.6657	4.9	0.2239	4.8	0.97	1302.5	56.1	1319.0	36.1	1319.0	21.9	1346.0	21.9	96.8
POR1-2-51	76	37895	2.1	11.5019	1.9	2.8487	3.5	0.2376	3.0	0.85	1374.4	37.0	1368.5	26.6	1359.2	36.3	1359.2	36.3	101.1
POR1-2-16	74	33450	2.8	11.2874	2.2	2.8771	4.6	0.2355	4.0	0.88	1363.4	49.6	1375.9	34.5	1395.4	41.3	1395.4	41.3	97.7
POR1-2-25	590	4977	1.3	11.1719	0.6	2.3222	4.5	0.1882	4.5	0.99	1111.4	45.9	1219.1	32.2	1415.1	11.9	1415.1	11.9	78.5
POR1-2-40	83	91152	4.3	10.7824	1.5	3.3106	4.8	0.2589	4.5	0.95	1484.2	59.8	1483.6	37.1	1482.6	28.5	1482.6	28.5	100.1
POR1-2-12	257	145813	2.4	10.5939	0.8	3.5202	2.6	0.2705	2.5	0.95	1543.2	34.5	1531.8	20.9	1516.0	15.1	1516.0	15.1	101.8
POR1-2-9	269	6481	2.6	10.5614	0.5	3.3099	5.7	0.2535	5.6	1.00	1456.7	73.5	1483.4	44.2	1521.8	8.8	1521.8	8.8	95.7
POR1-2-60	851	951777	2.6	9.9959	0.3	4.0079	3.9	0.2906	3.9	1.00	1644.3	55.9	1635.8	31.4	1624.8	5.6	1624.8	5.6	101.2
POR1-2-29	496	5282	3.8	9.9674	1.3	3.1377	4.6	0.2268	4.4	0.96	1317.9	52.6	1442.0	35.5	1630.1	24.9	1630.1	24.9	80.8
POR1-2-91	127	143332	1.1	9.8270	0.9	4.2567	4.2	0.3034	4.1	0.98	1708.								

Appendix 1. Table 2. POR 3-1 U-Pb geochronologic analyses.

Analysis	Isotope ratios										Apparent ages (Ma)								
	U (ppm)	206Pb/204Pb	U/Th	206Pb* ± 207Pb*	± 235U*	± 206Pb* ± 238U*	± error corr.	206Pb* ± 238U*	± error corr.	207Pb* ± 235U*	± error corr.	206Pb* ± 207Pb*	± error corr.	Best age (Ma)	± error corr.	Conc (%)			
POR3-1-74	358	35238	1.5	18.9990	3.6	0.4142	7.0	0.0571	6.0	0.86	357.8	21.0	351.9	20.9	313.1	82.6	357.8	21.0	NA
POR3-1-58	251	45070	2.3	18.9684	6.1	0.4284	6.6	0.0589	2.5	0.38	369.2	8.9	362.1	20.0	316.7	138.6	369.2	8.9	NA
POR3-1-79	246	42148	2.5	18.1402	4.9	0.4529	6.5	0.0596	4.3	0.66	373.1	15.7	379.3	20.7	417.3	110.0	373.1	15.7	NA
POR3-1-22	35	4077	2.5	14.8195	43.1	0.5595	44.0	0.0601	8.5	0.19	376.4	31.1	451.2	161.5	852.6	940.0	376.4	31.1	44.2
POR3-1-72	330	84428	6.6	17.8949	1.8	0.4698	8.9	0.0610	8.8	0.98	381.6	32.4	391.1	29.0	447.7	39.2	381.6	32.4	NA
POR3-1-71	853	83509	576.6	18.4178	1.3	0.4624	4.7	0.0618	4.6	0.96	386.4	17.1	385.9	15.2	383.3	29.5	386.4	17.1	NA
POR3-1-68	314	2675	1.4	17.0268	6.5	0.5154	10.7	0.0637	8.6	0.80	397.8	33.1	422.1	37.1	557.1	141.0	397.8	33.1	NA
POR3-1-39	662	1743	1.8	17.3128	2.1	0.5263	3.2	0.0661	2.4	0.75	412.5	9.6	429.3	11.2	520.7	46.5	412.5	9.6	NA
POR3-1-35	298	65142	3.5	18.1137	4.5	0.5086	5.2	0.0668	2.5	0.48	417.0	9.9	417.5	17.7	420.6	101.5	417.0	9.9	NA
POR3-1-29	223	39826	1.4	18.3927	3.5	0.5072	6.1	0.0677	5.0	0.82	422.0	20.6	416.6	21.0	386.4	79.2	422.0	20.6	NA
POR3-1-77	116	8268	2.9	17.7380	18.7	0.5434	19.4	0.0699	5.0	0.26	435.6	21.1	440.7	69.4	467.2	417.6	435.6	21.1	NA
POR3-1-99	521	4217	2.6	16.7096	3.9	0.5930	6.1	0.0719	4.7	0.76	447.4	20.2	472.8	23.1	598.0	85.6	447.4	20.2	74.8
POR3-1-16	261	54033	1.9	17.4223	6.5	0.5793	6.6	0.0732	1.2	0.18	455.4	5.3	464.0	24.5	506.8	142.3	455.4	5.3	NA
POR3-1-90	160	26212	1.6	17.3338	7.9	0.5993	11.0	0.0753	7.7	0.70	468.3	34.8	476.8	42.0	518.0	173.3	468.3	34.8	NA
POR3-1-98	261	4670	1.9	17.6478	7.4	0.6230	10.2	0.0797	7.1	0.69	494.5	33.7	491.7	39.8	478.5	163.0	494.5	33.7	NA
POR3-1-12	196	68830	3.2	16.9900	5.0	0.6930	5.2	0.0854	1.3	0.25	528.3	6.5	534.6	21.5	561.8	109.5	528.3	6.5	94.0
POR3-1-2	195	31510	1.1	17.1532	6.0	0.6978	6.3	0.0868	2.0	0.32	536.6	10.4	537.5	26.3	541.0	130.5	536.6	10.4	99.2
POR3-1-65	105	15682	2.0	16.8410	5.1	0.7301	5.7	0.0892	2.6	0.46	550.6	13.9	556.6	24.4	581.0	109.7	556.6	13.9	94.8
POR3-1-67	420	76342	3.0	17.1598	1.7	0.7449	5.9	0.0927	5.6	0.96	571.5	30.8	565.2	25.5	540.2	37.2	571.5	30.8	105.8
POR3-1-70	208	51550	1.6	16.7641	4.2	0.7645	5.5	0.0930	3.5	0.64	573.0	19.3	576.6	24.2	590.9	91.4	573.0	19.3	97.0
POR3-1-93	385	92880	2.5	16.7321	2.0	0.7791	3.3	0.0946	2.7	0.81	582.4	15.1	585.0	14.8	595.1	42.4	582.4	15.1	97.9
POR3-1-50	427	99717	1.4	16.7276	2.9	0.8197	5.6	0.0994	4.8	0.85	611.1	27.8	607.9	25.5	595.7	62.8	611.1	27.8	102.6
POR3-1-76	234	52074	0.9	16.8354	1.3	0.8180	3.3	0.0999	3.1	0.92	613.7	17.9	606.9	15.2	581.8	28.2	613.7	17.9	105.5
POR3-1-104	132	50249	1.4	16.1973	6.7	0.8661	7.3	0.1017	2.9	0.40	624.6	17.3	633.4	34.4	665.1	143.4	624.6	17.3	93.9
POR3-1-82	406	6945	0.5	16.1639	3.8	0.8711	5.0	0.1021	3.2	0.65	626.8	19.3	636.2	23.5	669.5	80.6	626.8	19.3	93.6
POR3-1-51	123	19785	1.6	16.5625	3.9	0.8547	6.5	0.1027	5.2	0.80	630.0	31.1	627.2	30.5	617.1	85.0	630.0	31.1	102.1
POR3-1-61	242	29031	1.4	16.1329	2.5	0.8868	3.7	0.1038	2.7	0.73	636.4	16.4	644.6	17.6	673.6	53.6	636.4	16.4	94.5
POR3-1-11	155	34754	3.5	16.7894	4.3	0.8554	5.5	0.1042	3.5	0.63	638.7	21.2	627.6	25.9	587.7	93.3	638.7	21.2	108.7
POR3-1-41	192	75137	2.9	14.4682	3.0	1.4887	5.6	0.1562	4.7	0.84	935.7	41.4	925.8	34.3	902.2	62.8	902.2	62.8	103.7
POR3-1-36	59	40864	0.9	14.0652	6.6	1.6911	7.2	0.1725	2.8	0.39	1025.9	26.7	1005.2	46.0	960.2	135.7	960.2	135.7	106.8
POR3-1-89	113	30428	1.4	14.0194	3.7	1.5328	5.2	0.1559	3.6	0.70	933.7	31.6	943.6	32.1	968.9	76.3	968.9	76.3	96.6
POR3-1-100	101	35082	3.8	13.9881	2.6	1.7000	4.3	0.1725	3.4	0.79	1025.7	32.0	1008.5	27.3	971.5	53.4	971.5	53.4	105.6
POR3-1-44	75	20306	1.1	13.9678	4.7	1.4766	5.2	0.1496	2.2	0.42	898.7	18.4	920.8	31.6	974.4	96.5	974.4	96.5	92.2
POR3-1-30	144	42243	2.8	13.9399	2.8	1.6418	5.8	0.1660	5.1	0.88	990.0	47.1	986.4	36.9	978.5	56.8	978.5	56.8	101.2
POR3-1-96	212	135713	2.5	13.8468	1.5	1.7322	4.5	0.1740	4.2	0.94	1033.9	40.5	1020.6	29.0	992.1	31.3	992.1	31.3	104.2
POR3-1-26	334	221003	5.9	13.5380	0.9	1.8426	3.0	0.1809	2.9	0.96	1072.0	28.8	1060.8	20.0	1037.8	17.3	1037.8	17.3	103.3
POR3-1-92	483	73404	5.4	13.5061	1.3	1.7866	7.4	0.1750	7.3	0.98	1039.6	70.1	1040.6	48.3	1042.5	26.4	1042.5	26.4	99.7
POR3-1-78	86	30889	3.9	13.5018	3.5	1.7662	6.7	0.1730	5.7	0.86	1028.4	54.4	1033.1	43.4	1043.2	69.8	1043.2	69.8	98.6
POR3-1-47	51	8414	1.5	13.4962	5.8	1.7658	7.1	0.1728	4.0	0.56	1027.8	37.7	1033.0	45.8	1044.0	118.1	1044.0	118.1	98.4
POR3-1-55	62	37929	2.1	13.4904	5.5	1.8233	6.8	0.1784	4.1	0.60	1058.2	40.3	1053.9	44.9	1044.9	110.0	1044.9	110.0	101.3
POR3-1-6	226	138726	2.8	13.4075	0.9	1.8754	2.1	0.1824	1.9	0.91	1079.9	19.0	1072.4	14.0	1057.4	18.0	1057.4	18.0	102.1
POR3-1-53	54	16328	2.7	13.3667	7.5	1.7475	8.2	0.1694	3.3	0.40	1008.9	30.8	1026.2	53.0	1063.5	151.2	1063.5	151.2	94.9
POR3-1-38	67	10693	0.9	13.2688	4.3	1.8876	5.7	0.1817	3.7	0.65	1076.0	36.6	1076.7	37.6	1078.2	86.4	1078.2	86.4	99.8
POR3-1-57	314	137957	2.8	13.2431	1.2	1.9224	3.8	0.1846	3.6	0.95	1092.3	36.2	1088.9	25.4	1082.1	24.2	1082.1	24.2	100.9
POR3-1-27	359	103801	3.2	13.1836	1.4	1.9995	3.5	0.1912	3.2	0.92	1127.8	33.4	1115.4	23.8	1091.1	27.5	1091.1	27.5	103.4
POR3-1-3	265	275580	2.1	13.0631	1.1	1.9894	3.0	0.1885	2.8	0.93	1113.1	28.6	1111.9	20.3	1109.5	22.5	1109.5	22.5	100.3
POR3-1-59	56	18473	1.8	12.9922	4.4	1.8916	5.6	0.1782	3.5	0.63	1057.4	34.5	1078.1	37.3	1120.4	87.0	1120.4	87.0	94.4
POR3-1-40	138	76897	2.7	12.7268	1.9	2.1534	3.9	0.1988	3.4	0.87	1168.7	36.1	1166.1	27.0	1161.4	38.5	1161.4	38.5	100.6
POR3-1-63	186	145079	3.4	12.6297	1.4	2.1554	6.7	0.1974	5.5	0.97	1161.5	58.7	1166.8	39.5	1176.6	27.2	1176.6	27.2	98.7
POR3-1-87	245	93423	2.5	12.4866	1.7	2.2441	5.4	0.2032	5.1	0.95	1192.7	56.0	1194.9	38.1	1199.1	33.9	1199.1	33.9	99.5
POR3-1-73	157	82652	1.5	12.4427	1.5	2.2687	4.0	0.2047	3.7	0.93	1200.7	40.8	1202.6	28.3	1206.0	29.3	1206.0	29.3	99.6
POR3-1-97	159	85639	3.1	12.4059	1.3	2.2585	3.2	0.2032	2.9	0.92	1192.5	31.6	1199.4	22.3	1211.9	25.1	1211.9	25.1	98.4
POR3-1-54	605	31974	1.3	11.9748	0.8	2.5919	4.5	0.2251	4.4	0.98	1308.8	52.2	1298.4	32.8	1281.1	15.9	1281.1	15.9	102.2
POR3-1-83	71	48315	3.2	11.9566	3.8	2.3170	8.7	0.2009	7.8	0.90	1180.3	84.0	1217.5	61.5	1284.1	73.9	1284.1	73.9	91.9
POR3-1-46	176	85134	3.1	11.9075	0.7	2.5296	1.8	0.2185	1.6	0.92	1273.7	18.7	1280.6	12.8	1292.1	13.3	1292.1	13.3	98.6
POR3-1-105	801	11417	4.0	11.8933	0.9	1.9534	2.0	0.1685	1.7	0.88	1003.8	16.2	1099.6	13.2	1294.4	17.8	1294.4	17.8	77.5
POR3-1-23	25	14540	2.3	11.8834	9.1	2.5340	9.9	0.2184	4.0	0.40	1273.4	46.3	1281.9	72.4	1296.0	176.9	1296.0	176.9	98.3
POR3-1-20	289	101885	2.6	11.8002	0.6	2.5733	1.2	0.2202	1.0	0.86	1283.1	12.2	1293.1	8.9	1309.7	12.0	1309.7	12.0	98.0
POR3-1-75	133	59123	3.2	11.7295	3.2	2.6047	5.7	0.2216	4.7	0.83	1290.2	54.9	1302.0	41.8	1321.3	62.3	1321.3	62.3	97.6
POR3-1-80	57	29658	0.8	11.6715	3.6	2.8136	6.2	0.2382	5.1	0.82	1377.2	63.3	1359.2	46.6	1330.9	68.8	1330.9	68.8	103.5
POR3-1-88	66	21230	1.8	11.6510	4.1	2.7396	7.0	0.2315	5.7	0.81	1342.3	69.1	1339.3	52.3	1334.3				

Appendix 1. Table 3. POR 4-1 U-Pb geochronologic analyses.

Analysis	Isotope ratios										Apparent ages (Ma)						Best age (Ma)	Conc (%)	
	U (ppm)	206Pb/204Pb	U/Th	206Pb*/207Pb*	±	207Pb*/235U*	±	206Pb*/238U*	±	error	206Pb*/238U*	±	207Pb*/235U*	±	206Pb*/207Pb*	±			
POR4-1-18	218	22817	2.2	19.4969	8.5	0.2953	9.7	0.0418	4.7	0.48	263.8	12.1	262.8	22.4	253.9	195.5	263.8	12.1	NA
POR4-1-52	559	32290	5.5	18.6281	3.2	0.3345	5.4	0.0452	4.3	0.80	284.9	12.1	293.0	13.8	357.7	73.3	284.9	12.1	NA
POR4-1-31	442	2521	2.3	18.2579	8.1	0.4094	9.5	0.0542	5.0	0.52	340.3	16.5	348.4	28.1	402.9	181.8	340.3	16.5	NA
POR4-1-24	207	25564	1.5	19.5606	8.0	0.4110	8.3	0.0583	2.4	0.28	365.3	8.4	349.6	24.6	246.4	184.1	365.3	8.4	NA
POR4-1-60	193	56643	1.5	18.0346	9.0	0.4666	9.3	0.0610	2.2	0.24	381.9	8.1	388.9	30.0	430.3	201.4	381.9	8.1	NA
POR4-1-11	228	27076	2.3	19.8770	9.2	0.4295	10.3	0.0619	4.7	0.45	387.3	17.5	362.8	31.3	209.3	212.6	387.3	17.5	NA
POR4-1-84	411	7987	1.4	17.1473	9.9	0.5042	11.6	0.0627	6.0	0.52	392.0	23.0	414.5	39.6	541.7	217.5	392.0	23.0	NA
POR4-1-89	208	27687	1.4	17.9636	7.4	0.4858	8.3	0.0633	3.7	0.45	395.6	14.4	402.0	27.6	439.1	164.9	395.6	14.4	NA
POR4-1-90	263	79791	0.8	17.8422	4.0	0.5055	8.1	0.0654	7.1	0.87	408.4	28.1	415.4	27.7	454.3	88.0	408.4	28.1	NA
POR4-1-30	284	46085	2.1	17.6394	15.1	0.5236	20.4	0.0670	13.6	0.67	418.0	55.1	427.6	71.1	479.5	336.2	418.0	55.1	NA
POR4-1-3	317	72093	1.9	18.4981	3.8	0.5011	4.2	0.0672	1.9	0.45	419.5	7.6	412.5	14.2	373.5	84.6	419.5	7.6	NA
POR4-1-68	882	216545	1.0	18.2457	1.7	0.5102	3.2	0.0675	2.7	0.84	421.2	11.1	418.6	11.1	404.4	39.1	421.2	11.1	NA
POR4-1-13	403	54810	1.1	18.0979	4.7	0.5192	5.1	0.0682	2.1	0.41	425.0	8.6	424.7	17.8	422.5	104.4	425.0	8.6	NA
POR4-1-28	474	112396	1.7	18.1350	2.3	0.5195	4.1	0.0683	3.3	0.82	426.1	13.7	424.8	14.1	418.0	52.2	426.1	13.7	NA
POR4-1-36	353	31841	1.3	17.5602	3.2	0.5453	6.9	0.0694	6.2	0.89	432.8	25.8	441.9	24.8	489.5	70.2	432.8	25.8	NA
POR4-1-81	104	33736	1.0	18.4775	12.0	0.5242	12.9	0.0703	4.7	0.37	437.7	19.9	428.0	44.9	376.0	269.8	437.7	19.9	NA
POR4-1-12	311	31951	0.8	17.8774	2.9	0.5436	4.8	0.0705	3.8	0.79	439.1	15.9	440.8	17.0	449.8	65.1	439.1	15.9	NA
POR4-1-70	136	18010	2.7	20.0784	7.7	0.4867	8.6	0.0709	3.9	0.45	441.4	16.6	402.7	28.5	185.9	178.3	441.4	16.6	NA
POR4-1-82	210	44313	3.3	17.0344	3.9	0.5954	7.6	0.0736	6.5	0.86	457.5	28.8	474.3	28.8	556.2	84.9	457.5	28.8	82.3
POR4-1-7	228	21806	1.9	17.1969	3.2	0.6031	4.5	0.0752	3.2	0.71	467.6	14.5	479.2	17.3	535.4	70.1	467.6	14.5	87.3
POR4-1-71	138	18385	1.3	17.1786	2.8	0.7329	7.4	0.0913	6.9	0.93	563.3	37.0	558.2	31.8	537.7	61.3	563.3	37.0	104.7
POR4-1-62	205	48615	2.0	16.3831	3.6	0.8071	4.6	0.0959	2.9	0.62	590.3	16.1	600.8	21.0	640.6	78.5	590.3	16.1	92.2
POR4-1-79	143	37292	1.0	16.3657	6.3	0.8380	7.1	0.0995	3.2	0.45	611.3	18.7	618.0	32.8	642.9	135.7	611.3	18.7	95.1
POR4-1-25	107	6935	1.9	16.4444	7.2	0.8349	7.8	0.0996	3.1	0.39	611.9	18.0	616.3	36.2	632.6	155.1	611.9	18.0	96.7
POR4-1-17	111	24018	1.6	15.9679	5.5	0.8755	5.9	0.1014	2.2	0.37	622.6	12.9	638.6	28.0	695.6	116.9	622.6	12.9	89.5
POR4-1-2	80	18291	3.2	15.7127	7.0	0.9045	8.3	0.1031	4.5	0.54	632.4	27.1	654.1	40.3	729.8	149.0	632.4	27.1	86.7
POR4-1-14	497	179449	1.3	16.4085	1.0	0.8662	4.4	0.1031	4.3	0.98	632.4	25.9	633.5	20.8	637.3	20.7	632.4	25.9	99.2
POR4-1-21	200	57046	0.8	16.4106	4.7	0.8662	5.9	0.1031	3.7	0.62	632.5	22.1	633.5	27.9	637.0	100.2	632.5	22.1	99.3
POR4-1-54	90	27006	0.6	16.3633	5.3	0.8816	6.9	0.1046	4.3	0.63	641.5	26.2	641.8	32.6	643.2	114.8	641.5	26.2	99.7
POR4-1-87	251	106000	0.9	16.3420	4.1	0.8844	5.0	0.1048	2.9	0.57	642.6	17.5	643.4	23.7	646.0	87.4	642.6	17.5	99.5
POR4-1-42	322	8177	1.6	16.2903	2.9	0.8912	3.3	0.1053	1.6	0.47	645.4	9.6	647.0	15.9	652.8	62.8	645.4	9.6	98.9
POR4-1-44	84	43747	2.9	14.2257	4.0	1.5637	5.1	0.1613	3.2	0.62	964.2	28.5	955.9	31.7	937.0	82.1	937.0	82.1	102.9
POR4-1-19	35	1900	1.2	13.9643	9.3	1.6033	16.1	0.1624	13.2	0.82	970.0	118.9	971.5	101.2	974.9	189.3	974.9	189.3	99.5
POR4-1-55	161	140061	3.4	13.8407	1.3	1.7007	4.7	0.1707	4.5	0.96	1016.1	42.0	1008.8	29.8	993.0	27.1	993.0	27.1	102.3
POR4-1-6	116	69410	1.5	13.7612	3.0	1.7026	4.3	0.1699	3.0	0.71	1011.7	28.3	1009.5	27.3	1004.7	61.2	1004.7	61.2	100.7
POR4-1-33	122	15146	2.6	13.6521	2.2	1.6774	2.9	0.1661	1.8	0.64	990.5	16.8	1000.0	18.3	1020.8	44.9	1020.8	44.9	97.0
POR4-1-4	80	35570	0.9	13.6014	3.9	1.7860	5.2	0.1762	3.4	0.66	1046.1	32.9	1040.4	33.6	1028.4	78.3	1028.4	78.3	101.7
POR4-1-76	916	363084	14.6	13.5337	0.9	1.7577	2.8	0.1725	2.7	0.95	1026.0	25.5	1030.0	18.3	1038.4	17.9	1038.4	17.9	98.8
POR4-1-63	279	43660	3.6	13.5162	1.4	1.7528	3.7	0.1718	3.4	0.92	1022.2	32.2	1028.2	23.8	1041.0	28.4	1041.0	28.4	98.2
POR4-1-61	106	43856	3.6	13.4503	3.1	1.7558	5.8	0.1713	5.0	0.85	1019.2	46.7	1029.3	37.7	1050.9	61.6	1050.9	61.6	97.0
POR4-1-66	316	164656	1.3	13.4211	1.3	1.8318	2.9	0.1783	2.6	0.89	1057.7	25.2	1056.9	19.0	1055.3	26.0	1055.3	26.0	100.2
POR4-1-64	137	68386	4.5	13.3363	3.1	1.8097	4.3	0.1750	2.9	0.69	1039.8	28.1	1049.0	27.8	1068.1	62.1	1068.1	62.1	97.4
POR4-1-58	82	29779	1.1	13.2716	3.9	1.8114	5.7	0.1744	4.1	0.72	1036.1	39.2	1049.6	37.1	1077.8	78.9	1077.8	78.9	96.1
POR4-1-49	605	12373	6.0	13.1483	0.9	1.9132	1.6	0.1824	1.3	0.82	1080.3	13.2	1085.7	10.8	1096.5	18.4	1096.5	18.4	98.5
POR4-1-20	139	292807	2.0	13.1445	2.1	1.9635	3.4	0.1872	2.6	0.78	1106.1	26.9	1103.1	22.8	1097.1	42.5	1097.1	42.5	100.8
POR4-1-37	315	109975	4.1	13.1339	1.4	2.1063	6.1	0.2006	5.9	0.97	1178.8	64.1	1150.9	42.1	1098.7	27.9	1098.7	27.9	107.3
POR4-1-73	200	76369	3.7	13.0746	0.9	2.0568	4.9	0.1950	4.8	0.98	1148.6	50.1	1134.6	33.2	1107.8	18.7	1107.8	18.7	103.7
POR4-1-27	112	50819	1.8	12.9559	2.3	2.0810	4.1	0.1955	3.4	0.83	1151.3	35.8	1142.6	28.1	1126.0	45.4	1126.0	45.4	102.2
POR4-1-22	75	56942	2.7	12.9419	4.9	2.0809	5.7	0.1953	2.8	0.50	1150.1	29.9	1142.5	38.9	1128.1	98.0	1128.1	98.0	101.9
POR4-1-23	164	61034	3.1	12.9026	2.2	2.0844	3.0	0.1951	2.1	0.69	1148.7	22.1	1143.7	20.8	1134.2	43.7	1134.2	43.7	101.3
POR4-1-99	116	57483	3.1	12.8558	3.3	2.0641	6.5	0.1925	5.5	0.86	1134.7	57.5	1137.0	44.2	1141.4	66.3	1141.4	66.3	99.4
POR4-1-59	133	38403	2.6	12.7789	2.4	2.0823	5.5	0.1930	5.0	0.90	1137.6	51.6	1143.0	37.8	1153.3	47.9	1153.3	47.9	98.6
POR4-1-105	180	73417	4.3	12.7778	1.7	2.1204	4.4	0.1965	4.0	0.92	1156.5	42.8	1155.5	30.2	1153.5	33.6	1153.5	33.6	100.3
POR4-1-80	66	44902	1.5	12.7711	3.6	2.0287	5.3	0.1879	3.9	0.74	1110.0	40.2	1125.2	36.2	1154.5	70.8	1154.5	70.8	96.1
POR4-1-48	193	143647	3.9	12.7337	1.6	2.0505	2.4	0.1894	1.8	0.75	1118.0	18.5	1132.5	16.3	1160.3	31.1	1160.3	31.1	96.3
POR4-1-32	42	29552	3.7	12.7004	4.5	2.1260	5.4	0.1958	3.0	0.56	1119.9	31.6	1157.3	37.1	1165.5	88.4	1165.5	88.4	98.9
POR4-1-9	77	15681	0.8	12.5775	8.6	2.4160	10.7	0.2204	6.4	0.60	1284.0	74.1	1247.4	76.8	1184.8	169.6	1184.8	169.6	108.4
POR4-1-16	33	14930	1.2	12.3027	5.0	1.9331	6.5	0.1725	4.2	0.64	1025.8	39.5	1092.6	43.8	1228.3	99.0	1228.3	99.0	83.5
POR4-1-29	122	28660	2.8	12.1399	1.5	2.4313	4.5	0.2141	4.3	0.94	1250.4	48.4	1251.9	32.6	1254.3	30.1	1254.3	30.1	99.7
POR4-1-1	127	60402	3.2	11.9674	1.2	2.5109	4.2	0.2179	4.0	0.95	1270.9	45.8	1275.2	30.2	1282.3	24.2	1282.3	24.2	99.2
POR4-1-98	31	21694	2.3	11.4720	4.6	2.9962	4.9	0.2493	1.7	0.35	1434.8	21.7	1406.7	37.0	1364.2	87.8	136		



*Current Research in Earth Sciences* is a peer-reviewed publication of the Kansas Geological Survey, a division of the University of Kansas. Each annual issue of this bulletin contains short articles about earth-science research in the midcontinent (North Dakota, South Dakota, Nebraska, Kansas, Oklahoma, Minnesota, Iowa, Missouri).

As part of the KGS Bulletin series, *Current Research in Earth Sciences* has national and international circulation. Manuscripts are expected to be of high quality. Articles submitted to this bulletin will be published online following peer review, revision, acceptance, and editing. KGS Bulletins are archived electronically.

Submission information: <http://www.kgs.ku.edu/Current/submit.html>

Kansas Geological Survey  
1930 Constant Avenue  
The University of Kansas  
Lawrence, KS 66047-3724  
785.864.3965

<http://www.kgs.ku.edu/>